

Influence of structural setting on sulphur isotopes in Archean orogenic gold deposits, Eastern Goldfields Province, Yilgarn, Western Australia

P. F. Hodkiewicz · D. I. Groves · G. J. Davidson ·
R. F. Weinberg · S. G. Hagemann

Received: 12 September 2008 / Accepted: 22 September 2008
© Springer-Verlag 2008

Abstract The published mean $\delta^{34}\text{S}$ values of ore-related pyrites from orogenic gold deposits of the Eastern Goldfields Province, Yilgarn Craton lie between -4% and $+4\%$. As for orogenic gold deposits worldwide, most deposits have positive means and a restricted range of $\delta^{34}\text{S}$ values, but some have negative means and wider ranges of $\delta^{34}\text{S}$ values. Wall-rock carbonation and back-mixing of similar-source fluids with different fluid pathways can explain some of the more negative $\delta^{34}\text{S}$ signatures. However, structural setting appears to be the most important factor controlling ore-fluid oxidation state and hence the distribution of $\delta^{34}\text{S}$ values in gold-related pyrites. Shear-hosted deposits appear to have experienced fluid-dominated processes such as phase separation, whereas stockwork,

vein-hosted or disseminated deposits formed under conditions of greater rock buffering. At Victory-Defiance, in particular, negative $\delta^{34}\text{S}$ values are more common in gently dipping dilational structures, compared to more compressional steeply dipping structures. It appears most likely that fluid-pressure fluctuations during fault-valve cycles establish different fluid-flow regimes in structures with different orientations. Rapid fluid-pressure fluctuations in dilational structures during seismic activity can cause partitioning of reduced gas phases from the ore fluid during extreme phase separation and hence are an effective method of ore-fluid oxidation, leading to large, local fluctuations in oxidation state. It is thus not necessary to invoke mixing with oxidised magmatic fluids to explain $\delta^{34}\text{S}$ signatures indicative of oxidation. In any case, available, robust geochronology in the Eastern Goldfields Province does not support the direct involvement of oxidised magmatic fluids from adjacent granitic intrusions in orogenic gold genesis. Thus, negative mean $\delta^{34}\text{S}$ values and large variations in $\delta^{34}\text{S}$ values of ore-related pyrites in world-class orogenic gold deposits are interpreted to result from multiple mechanisms of gold precipitation from a single, ubiquitous ore fluid in varying structural settings, rather than from the involvement of oxidised ore fluids from a different source. Such signatures are indicative, but not diagnostic, of anomalously large orogenic gold systems.

Editorial handling: P. Williams

Electronic supplementary material The online version of this article (doi:10.1007/s00126-008-0211-5) contains supplementary material, which is available to authorized users.

P. F. Hodkiewicz · D. I. Groves · S. G. Hagemann
Centre for Exploration Targeting, University of Western Australia,
35 Stirling Highway,
Crawley, Western Australia 6009, Australia

P. F. Hodkiewicz (✉)
SRK Consulting,
10 Richardson Street,
West Perth, Western Australia 6005, Australia
e-mail: phodkiewicz@srk.com.au

G. J. Davidson
School of Earth Sciences, University of Tasmania,
Private Bag 79,
Hobart, Tasmania 7001, Australia

R. F. Weinberg
School of Geosciences, Monash University,
Building 28,
Clayton, Victoria 3800, Australia

Keywords Archean · Yilgarn · Orogenic lode gold · Sulphur isotopes

Introduction

Sulphides in orogenic gold deposits typically have sulphur isotopic compositions ($\delta^{34}\text{S}$) ranging from 0% to $+9\%$ (McCuaig and Kerrich 1998) that are typically interpreted

to be the product of precipitation from a dominantly reduced ore fluid with a homogeneous isotopic composition. Several of the giant, and many world-class, orogenic gold deposits appear to have been deposited from reduced ore fluids and have restricted ranges of $\delta^{34}\text{S}$ values (e.g. Ashanti, Homestake, Ballarat, Bendigo: summarised by Groves et al. 2003). However, some giant orogenic gold deposits (e.g. Golden Mile, Timmins and Kirkland Lake) have much larger $\delta^{34}\text{S}$ ranges in gold-related pyrites, which have previously been interpreted to imply either mixture of sulphur from several disparate sources under reduced conditions at the site of ore formation or precipitation from a single sulphur source under more oxidising conditions (Ohmoto and Rye 1979). Cameron and Hattori (1987) proposed that oxidised fluids were responsible for the anomalously large gold endowment in these deposits. Whether the ore fluids were originally oxidised (e.g. through magmatic volatiles) or whether they became oxidised through ore-depositional processes (i.e. fluid–rock reaction, phase separation and/or fluid mixing) is a highly controversial issue in genetic models of orogenic gold-deposit formation (Phillips et al. 1986, 1996; Cameron and Hattori 1987; Hattori 1987; Cameron 1988; Kerrich 1989; Walshe et al. 1999; Ridley and Diamond 2000; Hall et al. 2001; Groves et al. 2003; Neumayr et al. 2005; Evans et al. 2006). This paper focusses on orogenic gold deposits of variable size and style in the Eastern Goldfields Province of the Yilgarn Craton. Its aim is to determine whether the large ranges of $\delta^{34}\text{S}_{(\text{py})}$ values are an indication of different fluid sources or of variations in gold-depositional processes and whether they can be directly related to the formation of world-class orogenic gold deposits. Our approach is to draw conclusions from the regional relationships between sulphur isotope variability and deposit characteristics (hydrothermal alteration assemblages, ore-fluid composition and structural style of mineralisation) over a range of deposit sizes. One deposit, Victory-Defiance, is evaluated in more detail.

Gold in orogenic deposits occurs most commonly in close association with sulphide minerals, and most authors concur that it was transported in the ore fluid predominantly as a bisulphide complex (Seward 1973; Phillips and Groves 1983; Mikucki 1998; Loucks and Mavrogenes 1999). Therefore, sulphide to sulphur isotope ratios are useful for constraining ore-depositional processes (Ohmoto and Rye 1979). Sulphur isotopes in orogenic gold sulphides are a potentially sensitive indicator of ore-fluid oxidation state. Reduced sulphur complexes in neutral solutions are capable of transporting gold in high concentrations, and gold solubility increases with oxygen fugacity up to the boundary between reduced and oxidised sulphur species (Fig. 1). The solubility of gold decreases rapidly at higher oxygen fugacities, where sulphate is the dominant sulphur

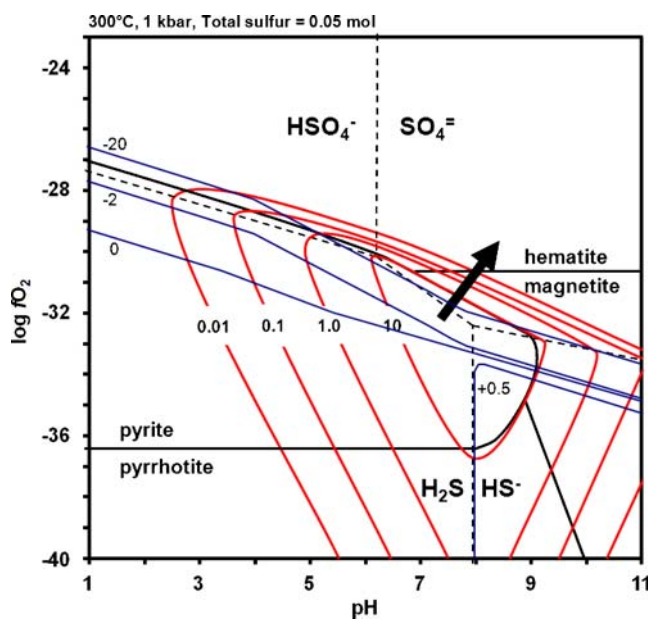


Fig. 1 Plot of oxygen fugacity ($\log f\text{O}_2$) against pH showing gold-solubility contours (0.01, 0.1, 1.0 and 10.0 ppm) for gold-bisulphide complexes, modified from Roberts (1987). Neutral solutions with low concentrations of total sulphur are capable of transporting gold in comparatively high concentrations as a sulphide complex. The solubility of gold in this state increases with $f\text{O}_2$ up to the boundary between the fields of reduced and oxidised sulphur. At higher oxygen fugacities, sulphate is the dominant species, and, with the decrease in the activity of the reduced sulphur species, the solubility of gold decreases markedly (see arrow). Therefore, oxidation of fluids is an efficient mechanism for the precipitation of gold. Isotopic contours are drawn as H_2S values. They were drawn with the aid of FO2PH (Zhang and Spry 1994), assuming $m\text{Na}^+=1$, $m\text{K}^+=0.1$ and $m\text{Ca}^{2+}=0.01$ and total $\delta^{34}\text{S}=0\text{‰}$

species in the ore fluid. Therefore, fluid oxidation is an efficient mechanism for gold precipitation (Roberts 1987). It also produces large sulphur isotopic fractionations between oxidised and reduced sulphur species, which is manifested as light $\delta^{34}\text{S}$ compositions in deposited sulphides (Fig. 1 and Ohmoto and Rye 1979). The magnitude of the fractionation is greater at lower temperatures and is also effectively greater at high sulphur activities because the pyrite stability field spans more of the fractionation range of dissolved H_2S (Ohmoto 1972). Under reducing conditions, where H_2S is the dominant aqueous sulphur species (see pyrite and pyrrhotite stability fields in Fig. 1), precipitated sulphides will have $\delta^{34}\text{S}$ values that are very similar to the sulphur in the ore fluid.

Sulphur in Archean orogenic ore fluids could have been derived from three sources: (1) pre-existing sulphides in the host greenstone sequences or in subducted or subcreted oceanic crust, (2) sulphur-bearing magmatic volatiles or (3) dissolved sulphur in seawater (Kerrich 1986). Sulphides in komatiite-hosted nickel deposits and sedimentary, mafic and ultramafic rocks in the Yilgarn Craton, which represent

the most likely major sulphur reservoirs prior to gold mineralisation, have published $\delta^{34}\text{S}$ values that are generally in a restricted range from +1‰ to +5‰ (Donnelly et al. 1978; Seccombe et al. 1981; Lambert et al. 1984). Sulphur in magmas usually has $\delta^{34}\text{S}$ values near 0 (Ohmoto and Rye 1979), but magmatic fluids derived from them may be reduced or oxidised depending on the oxidation state of the magmas, and extensive open-system degassing can lead to local enrichment of ^{34}S (Marini et al. 1998). Ohmoto and Goldhaber (1997) suggest that Archean seawater sulphate had $\delta^{34}\text{S}$ values between 2‰ and 10‰.

The range of $\delta^{34}\text{S}$ values from these potential sulphur sources, excluding oxidised magmatic fluids, is approximately 0‰ to +10‰, which is similar to the range of $\delta^{34}\text{S}$ values in ore-related sulphides in most Archean orogenic gold deposits (e.g. McCuaig and Kerrich 1998). Therefore, determining the source of sulphur in Archean orogenic gold fluids, based on $\delta^{34}\text{S}$ values in sulphide minerals, is normally impossible because of the overlapping $\delta^{34}\text{S}$ ranges from the potential sources. It is a key premise of this paper that only sulphides with anomalously negative $\delta^{34}\text{S}$ can potentially provide clues to source and/or anomalous ore-fluid behaviour at the depositional site.

Sulphides analysed in this study

Sample selection

A total of 78 samples from 20 deposits in the Eastern Goldfields Province were analysed for this study and combined with results from previous studies (Table 1). All samples are from well-documented Ph.D. and B.Sc. Honours collections at the Edward de Courcy Clarke Geological Museum at the University of Western Australia.

Samples were selected to determine broad relationships between sulphur isotope variability and deposit characteristics such as hydrothermal alteration assemblages, ore-fluid composition and structural style of mineralization, over a range of deposit sizes. In order to investigate the influence of structural style, deposits in this study were classified as either shear-hosted or stockwork–vein-hosted (Table 1). Gold deposits in the Eastern Goldfields Province occur in a wide variety of structural settings, so this broad classification is useful for distinguishing dominantly ductile (shear-hosted) deposits from dominantly brittle (stockwork–vein-hosted) deposits (Witt 1993). In shear-hosted deposits, gold mineralisation occurs mostly in shear zones that acted as major conduits for hydrothermal fluid flow during mineralisation (i.e. mineralisation is interpreted to have formed under fluid-dominated conditions). In stockwork–vein-hosted deposits, gold occurs mostly in brittle vein arrays and with associated disseminated sulphides in

hydrothermally altered wall rock (i.e. mineralisation is interpreted to have formed under conditions of greater rock buffering).

The Victory-Defiance deposit was selected for a case study because: (1) it is a world-class orogenic gold deposit, containing a pre-mining resource of approximately 250 t of gold; (2) gold mineralisation is hosted in a variety of rock types and structural styles (Clark et al. 1986); (3) it is known to have a large range of sulphur isotope values (Palin and Xu 2000); and (4) pyrite samples from the well-mineralised 32 Shear zone, the subject of a detailed lead isotope study by Ho et al. (1994), were available. Twenty-four samples from Victory-Defiance were analysed for this study.

Analytical techniques

Analytical techniques used in this study include both Nd-YAG laser ablation of in situ sulphides (Huston et al. 1995) and conventional techniques for pyrite separates (Robinson and Kusakabe 1975). All results are reported as $\delta^{34}\text{S}$ values in parts per thousand (per mil=‰), relative to Canyon Diabolo Triolite. A total of 99 in situ laser ablation analyses and 25 conventional analyses of pyrite separates were completed for this study. In this study, analytical precisions (1σ) are 0.22‰ for laser ablation and 0.05‰ for conventional methods. All analytical works were completed at the Central Science Laboratory and the ARC Centre of Excellence in Ore Deposits at the University of Tasmania. Results are provided in a [supplementary](#) electronic data archive.

Regional sulphur isotope study

Introduction

Sampled locations and analytical results from this study are summarised in Table 1 and Figs. 2 and 3. Eight deposits were selected from the regional study for a more detailed discussion in this section: six with positive average $\delta^{34}\text{S}_{(\text{py})}$ values and two with negative average $\delta^{34}\text{S}_{(\text{py})}$ values. For each of these cases, a brief overview of host rocks, structural style of mineralisation, ore-fluid characteristics and inferred ore-depositional mechanisms is shown in Table 2. Sulphur isotope values from each deposit are described below.

Deposits with positive average $\delta^{34}\text{S}_{(\text{py})}$ values

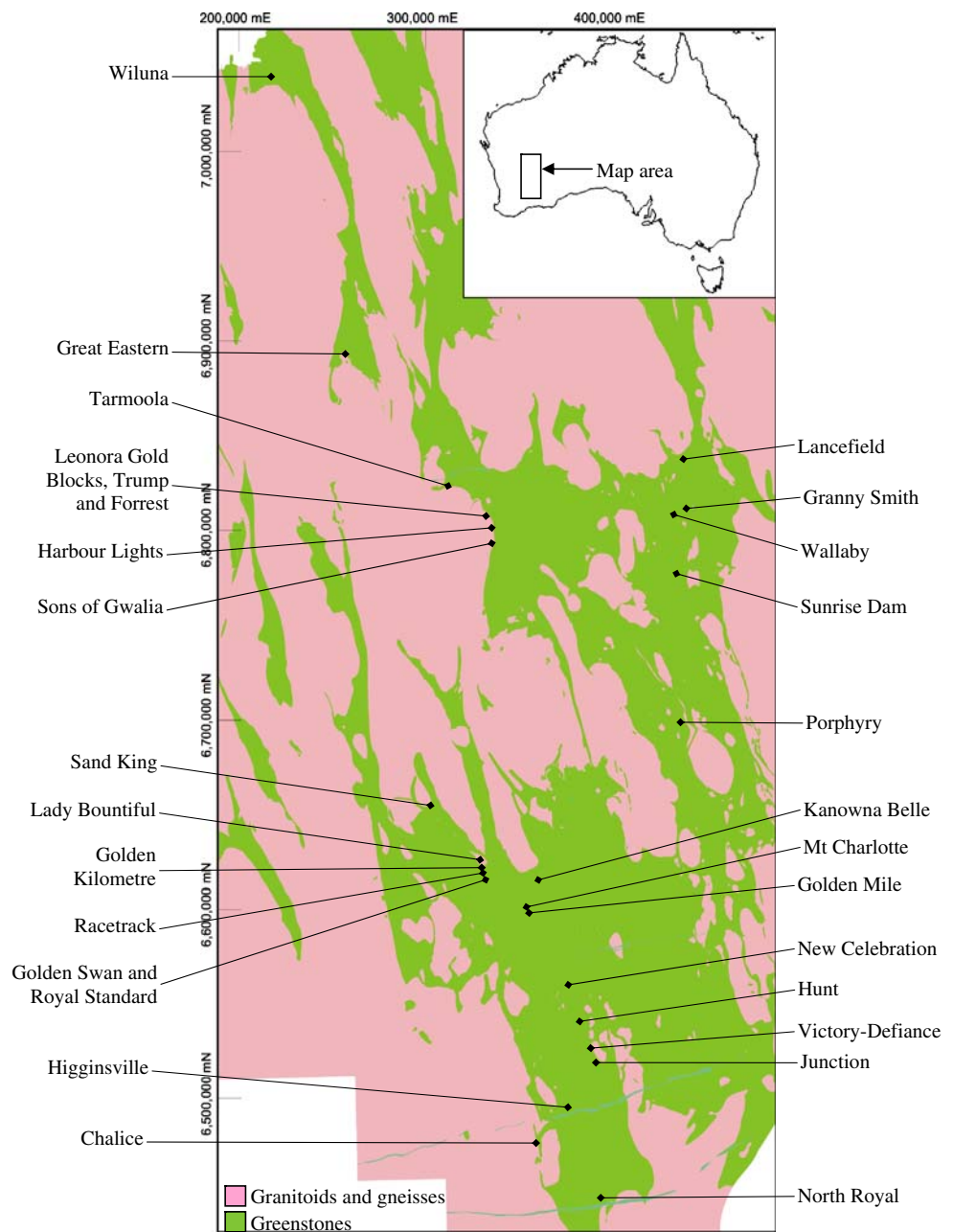
Deposits discussed in this section are Sunrise Dam, North Royal, Golden Kilometre, Great Eastern, Lady Bountiful and Hunt (Fig. 2) in order of decreasing size. Photographs

Table 1 List of gold deposits in the Eastern Goldfields Province, arranged from north to south. Deposit locations are shown in Fig. 2

Deposit name	Dominant structural style of mineralisation	Pre-mining endowment (tonnes Au)	Number of samples/analyses	Min and max $\delta^{34}\text{S}_{(\text{py})}$ ‰ values (total range)	References	Analytical methods
Wiluna	Stockwork/vein-hosted	86	10/10	-2.5 to +1.0 (3.5)	Hagemann (1992)	CONV
Great Eastern	Stockwork/vein-hosted	15	13/14	-0.6 to +2.5 (3.1)	This study; Mikucki (1997)	LA/ CONV
Tarmoola	Stockwork/vein-hosted	100	10/10	0.0 to +4.0 (4.0)	Duuring (2002)	CONV
Leonora Gold Blocks	Shear-hosted	1	1/1	+7.1	This study; Skwarnecki (1990)	LA
Trump Mine	Shear-hosted	1	1/2	+2.7 to +2.9 (0.2)	This study; Skwarnecki (1990)	LA
Forrest Mine	Shear-hosted	1	1/2	+0.6 to +2.6 (2.0)	This study; Skwarnecki (1990)	LA
Harbour Lights	Shear-hosted	10	2/3	-1.1 to +5.1 (6.2)	This study; Skwarnecki (1990)	LA
Sons of Gwalia	Shear-hosted	130	3/5	+0.7 to +3.2 (2.5)	This study; Skwarnecki (1990)	LA
Lancefield	Shear-hosted	46	18/18	-6.4 to +3.2 (9.6)	Hronsky (1993)	CONV
Granny Smith	Stockwork/vein-hosted	50	7/11	+0.3 to +4.5 (4.2)	Ojala (1995)	CONV
Wallaby	Stockwork/vein-hosted	200	6/9	-0.7 to +6.2 (6.9)	Salier et al. (2004, 2005)	LA
Sunrise Dam	Shear-hosted	250	19/21	-8.2 to +4.0 (12.2)	This study; Brown (2002)	LA/ CONV
Porphyry	Shear-hosted	11	13/19	-10.2 to +10.0 (20.2)	This study; Allen (1986)	LA
Sand King	Stockwork/vein-hosted	2	10/11	+0.9 to +6.0 (5.1)	This study; WMC (unpublished data)	LA/ CONV
Golden Kilometre	Stockwork/vein-hosted	17	8/13	-4.3 to +7.0 (11.3)	This study; Gebre-Mariam (1994)	LA/ CONV
Lady Bountiful	Stockwork/vein-hosted	11	9/14	-1.1 to +9.5 (10.6)	This study; Cassidy (1992)	LA/ CONV
Ora Banda	Stockwork/vein-hosted	18	1/2	+1.7 to +3.0 (1.3)	This study; Mueller (1990)	LA
Racetrack	Shear-hosted	13	5/6	+1.6 to +7.3 (5.7)	This study; Gebre-Mariam (1994)	LA/ CONV
Golden Swan	Stockwork/vein-hosted	1	1/2	+3.4 to +5.4 (2.0)	This study; Gebre-Mariam (1994)	LA
Royal Standard	Stockwork/vein-hosted	1	1/1	3.6	This study; Gebre-Mariam (1994)	LA
Kanowna Belle	Stockwork/vein-hosted	130	5/14	-5.4 to 10.9 (16.3)	Ross (2002)	LA
Mt. Charlotte	Stockwork/vein-hosted	160	34/34	-3.8 to +8.9 (12.7)	Clout (1989); Harbi (1997)	CONV
Golden Mile	Shear-hosted	2,500	224/224	-9.8 to 12.7 (22.5)	Clout (1989); Hagemann et al. (1999)	LA/ CONV
New Celebration	Shear-hosted	100	5/8	-8.6 to +5.5 (14.1)	This study; Williams (1994)	LA
Hunt	Shear-hosted	10	6/10	+1.0 to +8.0 (7.0)	This study; Lambert et al. (1984)	LA
Victory-Defiance	Shear-hosted	250	28/58	-6.3 to +5.1 (11.4)	This study; Palin and Xu (2000)	LA/ CONV
Junction	Stockwork/vein-hosted	60	6/6	+2.2 to +5.1 (2.9)	Polito (1999)	CONV
Higginsville	Shear-hosted	10	1/2	+7.3 to +7.9 (0.6)	This study; Cater (1992)	LA
Chalice	Shear-hosted	18	5/14	+1.8 to +3.5 (1.7)	Bucci (2001)	CONV
North Royal	Shear-hosted	55	4/9	+0.3 to +10.4 (10.1)	This study; Mueller (1990)	LA/ CONV

All $\delta^{34}\text{S}$ values are from ore-related pyrite. Pre-mining endowment figures are from Townsend et al. (2000). Analytical methods are listed: CONV is conventional and LA is laser ablation. Dominant structural styles of mineralisation are from listed references and deposit summaries in Vanderhor and Groves (1998)

Fig. 2 Simplified map of the Eastern Goldfields Province (from Groenewald and Riganti 2004), showing locations of deposits with sulphur isotope data from this study and previous studies. Data are shown in Table 1. Map grid is in AMG coordinates, in metres



of rock samples from these deposits, with $\delta^{34}\text{S}_{(\text{py})}$ values, are shown in Fig. 4. These deposits were selected because they have ore-related pyrites with dominantly positive average $\delta^{34}\text{S}$ values, based on results of this and previous studies, although several deposits also have ore-related pyrites with anomalously positive or negative $\delta^{34}\text{S}_{(\text{py})}$ values.

At *Sunrise Dam* (Table 2), the average $\delta^{34}\text{S}_{(\text{py})}$ value for gold-related pyrites is +1.1‰ (± 3.5), with a total range from -8.2‰ to +4.0‰, based on results from this study ($n=4$) and that of Brown (2002; $n=17$). The rare negative $\delta^{34}\text{S}_{(\text{py})}$ values occur in the more gently dipping Sunrise Shear Zone, where samples from a single magnetite-bearing

shale unit show a large difference in $\delta^{34}\text{S}_{(\text{py})}$ values, ranging from +2.5‰ (Fig. 4a) to -6.8‰ (Fig. 4b).

At *North Royal* (Table 2), the average of nine laser ablation $\delta^{34}\text{S}_{(\text{py})}$ analyses is +4.1‰ (± 3.0), from quartz veins and proximal wall-rock alteration halos. Eight values range from +0.3‰ to +5.8‰ and there is one anomalous value of +10.4‰ (Fig. 4c), from the transition zone between inner chlorite-biotite and outer chlorite-bearing alteration assemblages.

At *Golden Kilometre* (Table 2), the average $\delta^{34}\text{S}_{(\text{py})}$ value for gold-related pyrites is +3.2‰ (± 3.0), with a total range from -4.3‰ to +6.9‰ ($n=10$). This includes two values of +3.2‰ and +3.7‰ from Gebre-Mariam (1994).

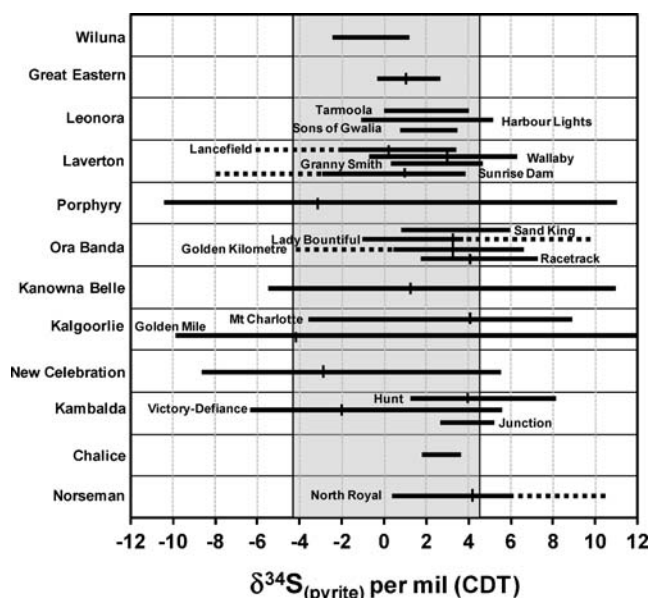


Fig. 3 Total range of $\delta^{34}\text{S}$ values in ore-related pyrites by deposit and average $\delta^{34}\text{S}_{(\text{py})}$ values (short vertical lines), arranged from north to south and corresponding to locations in Fig. 2. Labels along the left side include district, or gold-camp, names, where several ranges are shown. Dashed lines correspond to $\delta^{34}\text{S}_{(\text{py})}$ ranges based on limited data (i.e. one sample or analysis). The grey area corresponds to the range of average $\delta^{34}\text{S}_{(\text{py})}$ values based on analytical results of this study and data compiled from previous studies (see Table 1)

Of eight analyses from this study, seven values range from +2.6‰ to +6.9‰, with one anomalous value of -4.3‰ in a quartz vein, less than 10 mm from two pyrites with $\delta^{34}\text{S}$ values of +2.6‰ and +3.3‰ (Fig. 4d).

At *Great Eastern* (Table 2), the average $\delta^{34}\text{S}_{(\text{py})}$ value for gold-related pyrites is +0.9‰ (± 0.9), with a total range from -0.6‰ to +2.6‰ ($n=14$). Results of a previous conventional stable-isotope study show $\delta^{34}\text{S}_{(\text{py})}$ values of -0.6‰ to +2.1‰, with no apparent difference in values between the two mineralisation styles ($n=12$; Mikucki 1997). Results from this study include laser ablation analyses of two pyrites from a sample of late-stage chlorite-hematite, gold-telluride mineralisation, with $\delta^{34}\text{S}_{(\text{py})}$ values of +2.5‰ and +1.5‰ (Fig. 4e).

At *Lady Bountiful* (Table 2), the average of nine laser ablation and five conventional $\delta^{34}\text{S}_{(\text{py})}$ analyses is +3.2‰ (± 2.3), with a total range from -1.1‰ to +5.5‰ ($n=14$). This includes 13 values ranging from -1.1‰ to +4.8‰, in both quartz veins and proximal alteration halos, and one anomalous value of +9.5‰ in a mineralised quartz vein (Fig. 4f), which is hosted in granodiorite, near the contact with a layered sill (Cassidy 1992). The pyrite in the central portion of the vein has a $\delta^{34}\text{S}$ value of +3.6‰, whereas a pyrite grain 3 mm away near the vein margin has the anomalous $\delta^{34}\text{S}$ value of +9.5‰.

At *Hunt* (Table 2), the average $\delta^{34}\text{S}$ value in gold-related pyrites is +4.7‰ (± 1.5), with a total range from +3.4‰ to

+8.0‰ ($n=10$). Previous studies indicate a narrow range of $\delta^{34}\text{S}$ values from three gold-related pyrites (+4.4‰ to +8.0‰; Lambert et al. 1984). These are similar to new results from this study, with $\delta^{34}\text{S}_{(\text{py})}$ values ranging from +3.4‰ to +4.9‰ ($n=5$) in vein-related wall-rock alteration (Fig. 4g) and auriferous quartz veins (Fig. 4h).

Deposits with negative average $\delta^{34}\text{S}_{(\text{py})}$ values

Both the large *New Celebration* and small *Porphyry* deposits have negative average $\delta^{34}\text{S}$ values in ore-related pyrites.

At *New Celebration* (Table 2), $\delta^{34}\text{S}_{(\text{py})}$ values range from -8.6‰ to +5.5‰, with an average value of -3.0‰ (± 5.2). There is a large range in the tholeiitic mafic schist with pre-gold magnetite alteration, with $\delta^{34}\text{S}_{(\text{py})}$ values of -5.5‰ and -4.8‰ in proximal alteration and a value of +5.5‰ in distal alteration (Fig. 5). Negative $\delta^{34}\text{S}_{(\text{py})}$ values from the felsic porphyry unit with abundant pre-gold hematite alteration range from -8.6‰ to -6.0‰ in proximal alteration with a value of -1.4‰ in distal alteration. A sample of distal footwall ultramafic schist has a $\delta^{34}\text{S}_{(\text{py})}$ value of +3.9‰. There is a broad negative correlation between whole-rock gold values and pyrite $\delta^{34}\text{S}$ values (Table 3 and Fig. 6).

The small *Porphyry* deposit (Table 2) has an anomalously large range of $\delta^{34}\text{S}_{(\text{py})}$ values, from -10.2‰ to +10.0‰ ($n=19$), second only to the giant *Golden Mile* deposit (Clout 1989). The average value is -3.1‰ (± 5.8). The largest variations in $\delta^{34}\text{S}_{(\text{py})}$ values occur within, and adjacent to, the mineralised shear zones. More negative $\delta^{34}\text{S}_{(\text{py})}$ values correspond to higher gold grades (>3 g/t), more intense shear-fabric development and hematite alteration (Fig. 7a,b). With increasing distance from the lodes, gold grades, hematite alteration and shear-fabric development decrease and $\delta^{34}\text{S}_{(\text{py})}$ values increase, approaching 0‰ (Fig. 7c,d). Weakly mineralised samples adjacent to the lode have the most positive $\delta^{34}\text{S}$ values, approaching +10.0‰ (Fig. 7e,f). There is a broad negative correlation between whole-rock gold values and pyrite $\delta^{34}\text{S}$ values (Table 4 and Fig. 6).

Summary of regional study

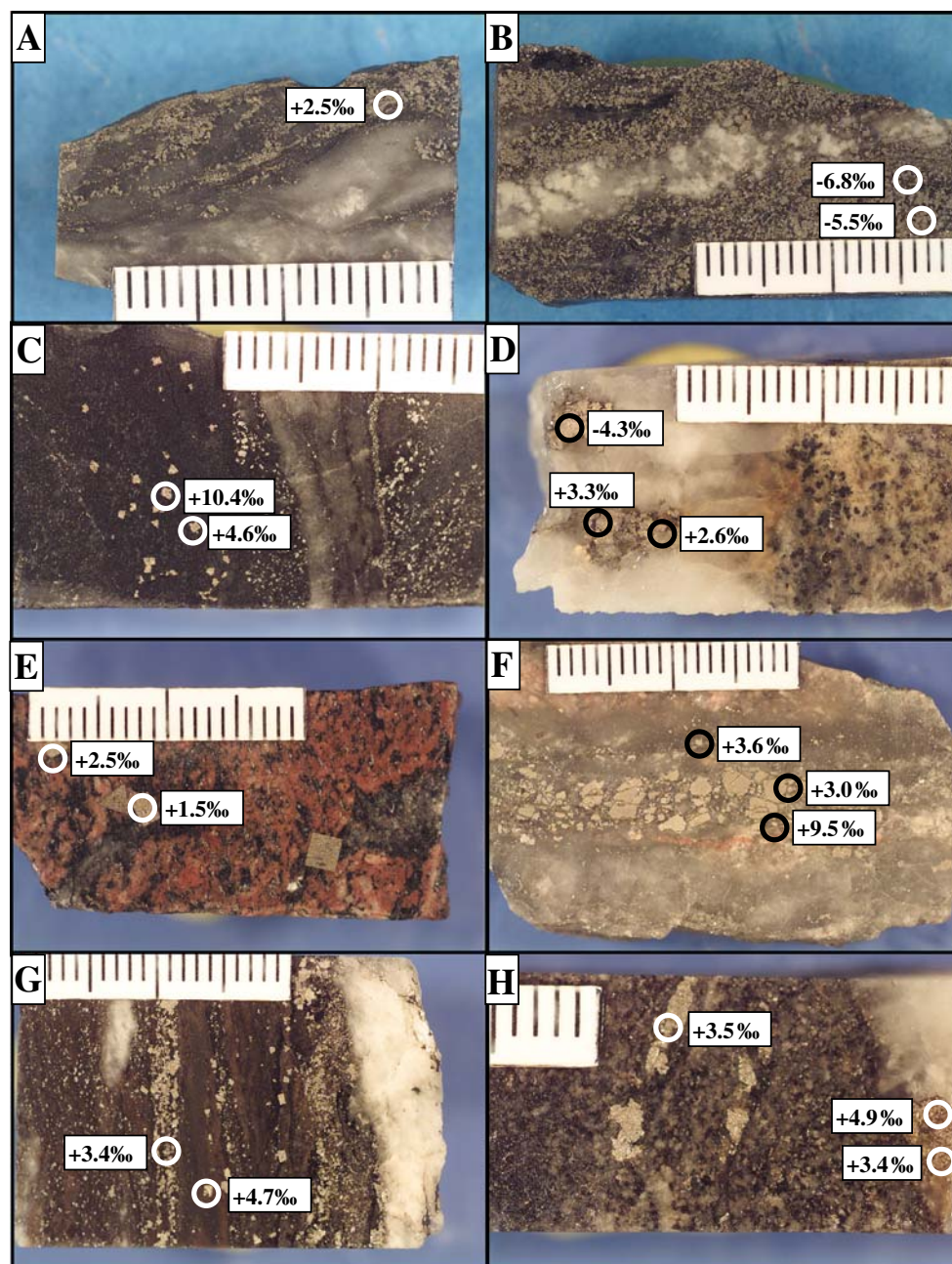
Analytical results and geological characteristics of the eight deposits in the regional study are summarised in Table 2. Six deposits have ore-related pyrites with positive average $\delta^{34}\text{S}$ values, ranging from 0.9‰ (± 0.9) at *Great Eastern* to 4.1‰ (± 3.0) at *North Royal*, whereas *Porphyry* has an average $\delta^{34}\text{S}_{(\text{py})}$ value of -2.1‰ (± 6.0) and *New Celebration* has an average $\delta^{34}\text{S}_{(\text{py})}$ value of -3.0‰ (± 5.2). In the last two deposits, there is also a larger and more consistent variation in $\delta^{34}\text{S}_{(\text{py})}$, with ranges of 20.2‰ at *Porphyry* and

Table 2 Summary of deposit characteristics and $\delta^{34}\text{S}$ values of ore-related pyrites from regional study of deposits in the Eastern Goldfields Province

Deposit	Pre-mining endowment (tonnes Au)	Max and min $\delta^{34}\text{S}_{\text{py}}$ ‰ values from this and previous studies, n =total number of analyses	Total range of $\delta^{34}\text{S}_{\text{py}}$ ‰ values	Mean $\delta^{34}\text{S}_{\text{py}}$ ‰ value and STD	Structural style of mineralisation	Host rocks	Ore-fluid characteristics	Inferred ore-depositional mechanisms	References
Sunrise Dam	250	-8.2 to +4.0 ($n=21$)	12.2	+1.1 (± 3.5)	Variably dipping brittle-ductile shear zones (Western Lodes $\sim 70^\circ$ and Sunrise Shear Zone $\sim 30^\circ$)	Felsic to intermediate volcanoclastic and sedimentary rocks, with thin magnetite-rich shale units and rhyodacite porphyry dikes	$\text{H}_2\text{O-CO}_2 \pm \text{CH}_4$, < 2 to 21 wt.% NaCl equivalent, 110–140 MPa, 280–320°C	Fluid-wall rock interaction and minor phase separation	Brown and Tomatona (2001); Brown (2002); Brown et al. (2002a, b)
North Royal	55	0.3 to +10.4 ($n=9$)	10.1	+4.1 (± 3.0)	Laminated quartz veins in steep to sub-vertical, brittle-ductile shear zones	Tholeiitic basalt and gabbroic dikes	CO_2 -rich, low salinity, <300 MPa, 420–475°C	Fluid-wall rock interaction and phase separation	McCuaig et al. (1993); McCuaig (1996)
Golden Kilometre	17	-4.3 to +3.4 ($n=10$)	7.7	+3.2 (± 3.0)	Brittle, laminated quartz-carbonate veins and breccias	Fe- and Ti-rich quartz gabbro	$\text{H}_2\text{O-CO}_2 \pm \text{CH}_4$, 3.7 wt.% NaCl equivalent, 50–190 MPa, 275 \pm 75°C	Fluid-wall rock interaction and phase separation	Witt (1992b); Gebre-Mariam (1994)
Great Eastern	15	-0.6 to +2.6 ($n=14$)	3.2	+0.9 (± 0.9)	Steep, brittle-ductile shear zones, brittle vein arrays and breccias	Tonalite, diorite and granodiorite	$\text{H}_2\text{O-CO}_2 \pm \text{CH}_4$, 3.5 to 7.9 wt.% NaCl equivalent, 50–200 MPa, >350°C	Fluid-wall rock interaction and mixing with surface water	Cassidy (1992); Mikucki (1997)
Lady Bountiful	11	-1.1 to +9.5 ($n=14$)	10.6	+3.2 (± 2.3)	Laminated quartz veins, brittle quartz vein arrays and breccias	Granodiorite, gabbro and quartz gabbro	$\text{H}_2\text{O-CO}_2 \pm \text{CH}_4$, 7 to 10 wt.% NaCl equivalent, 50–200 MPa, 200–350°C	Phase separation	Cassidy (1992); Cassidy and Bennett (1993)
Hunt	10	+1.0 to +8.0 ($n=10$)	7.0	+3.9 (± 2.0)	Steep (Subvertical to 70°), brittle-ductile shear zones	Low-Mg basalt, dolerite, komatite, felsic porphyry dikes	$\text{H}_2\text{O-CO}_2$, ~2 wt. % NaCl equivalent, 80–180 MPa, 280–350°C	Fluid-wall rock interaction	Lambert et al. (1984); Phillips and Groves (1984); Neall and Phillips (1987); Witt (1992a)
New Celebration	100	-8.6 to +5.5 ($n=8$)	14.1	-3.0 (± 5.2)	Steep to sub-vertical brittle-ductile shear zones	Mafic schist, talc chlorite schist and felsic porphyry dikes	$\text{H}_2\text{O-CO}_2 \pm \text{CH}_4$, 6 to 23 wt.% NaCl equivalent, 300–400 MPa, 300–450°C	Fluid-wall rock interaction	Williams (1994); Townsend et al. (2000); Hodge et al. (2005)
Porphyry	11	-10.2 to +10.0 ($n=19$)	20.2	-3.1 (± 5.8)	Gently dipping (20 to 25°) brittle-ductile shear zone	Quartz monzonite and minor quartz andesite	$\text{CO}_2\text{-H}_2\text{O}$ low salinity, 200 MPa, 350°C	Phase separation and minor fluid-rock interaction	Allen (1986, 1987); Cassidy (1992); Witt (1995); Cassidy et al. (1998)

The first six deposits, listed in order of decreasing gold endowment, have positive average $\delta^{34}\text{S}$ values, whereas the last two have negative average $\delta^{34}\text{S}$ values

Fig. 4 Sample photographs and $\delta^{34}\text{S}$ values of ore-related pyrites from deposits in the Eastern Goldfields Province. Analytical results are from this study. Scale bar is in millimetre increments. **a, b** Sunrise Dam samples from the Sunrise Shear Zone (Brown 2002). **c** North Royal sample from the transition zone between inner chlorite–biotite and outer chlorite-bearing alteration assemblages (Mueller 1990). **d** Golden Kilometre sample from the contact between a quartz vein and sericite–ankerite-altered gabbro (Mueller 1990). **e** Great Eastern sample from late-stage chlorite–hematite alteration, associated with gold–telluride mineralisation (Cassidy 1992). **f** Lady Bountiful sample from the Liberty Granodiorite, near the contact with the Mt. Ellis Sill (Cassidy 1992). **g** Hunt Mine sample from weakly mineralised pyrite–biotite–chlorite–ankerite schist from the 12 Level, 1221 east drive, A Fault (Mueller 1990). **h** Hunt Mine sample from strongly mineralised pyrite–biotite–ankerite schist from 10 Level, 1020 east drive, A Fault (Mueller 1990)



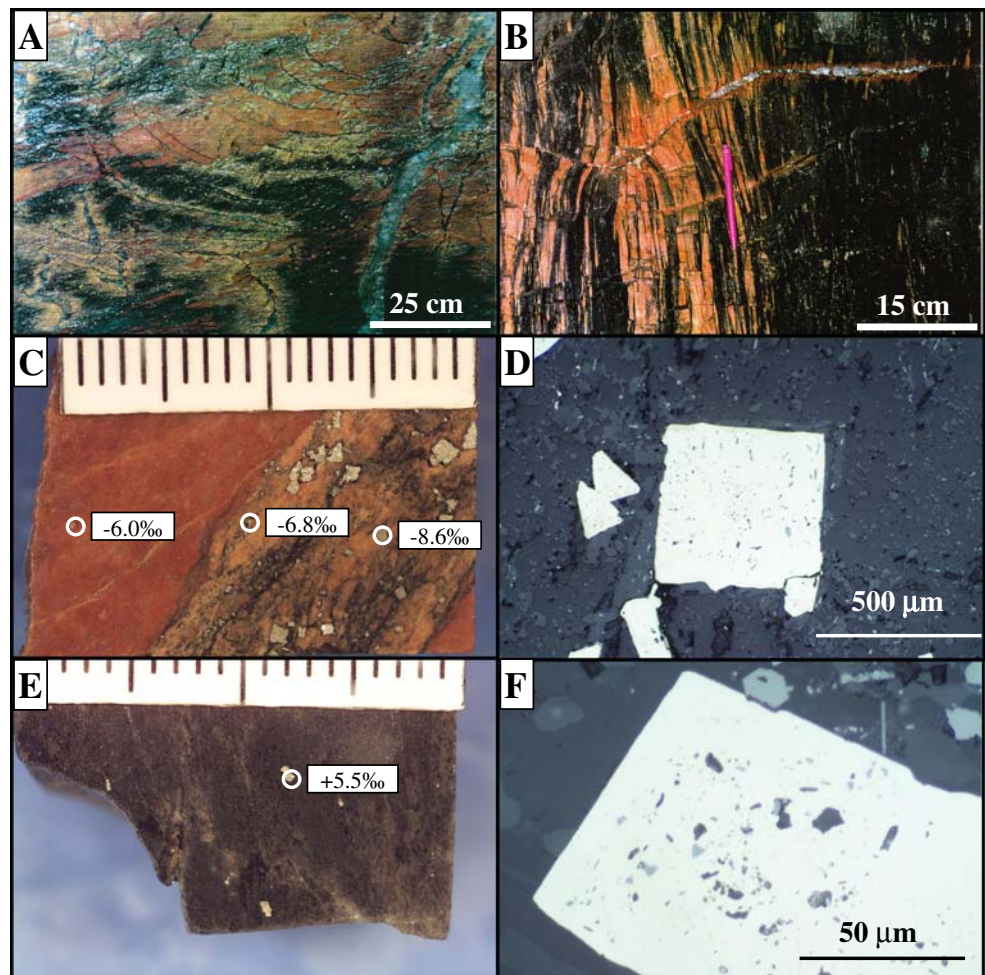
14.1‰ at New Celebration. At Sunrise Dam, there is also a relatively large range in $\delta^{34}\text{S}_{(\text{py})}$ (12.2‰), although the average value is +1.1 (± 3.5). The large range at Sunrise Dam is due to rare occurrences of negative $\delta^{34}\text{S}_{(\text{py})}$ values in magnetite-rich shales in the gently dipping Sunrise Shear Zone. Likewise, relatively large variations in $\delta^{34}\text{S}_{(\text{py})}$ values at Lady Bountiful (10.6‰) and North Royal (10.1‰) are the result of rare occurrences of pyrites with anomalously positive $\delta^{34}\text{S}$ values within and adjacent to veins. At Golden Kilometre, the single negative $\delta^{34}\text{S}_{(\text{py})}$ value from this study (−4.3‰) occurs in a vein.

A distinctive feature in the quartz–monzonite-hosted, gently dipping shear zones at Porphyry is the occurrence of ore-

related pyrites with negative $\delta^{34}\text{S}$ values in samples with higher gold grades and stronger hematite alteration. At New Celebration, mineralised pyrites with negative $\delta^{34}\text{S}$ values occur in sub-horizontal quartz–carbonate veins (Fig. 5a) that crosscut mafic schist, with abundant pre-gold magnetite alteration, and felsic porphyry dykes, with abundant pre-gold hematite alteration. A common feature is the association of negative $\delta^{34}\text{S}$ values with pre-gold Fe-oxide alteration, at least at New Celebration. At both Porphyry and New Celebration, there is also a broad negative correlation between whole-rock gold values and pyrite $\delta^{34}\text{S}$ values (Fig. 6).

There are no obvious explanations, in terms of any one measurable component, for the variations in $\delta^{34}\text{S}$

Fig. 5 Photographs of host rocks from the New Celebration deposit. Scale bar in c and e is in millimetre increments. **a** Underground mine exposure of mineralised quartz–carbonate \pm pyrite veins, with yellow feldspar–ankerite–pyrite selvages, crosscutting dark tholeiitic mafic schist with pre-gold magnetite alteration and orange felsic porphyry with pre-gold hematite alteration (from Williams 1994). **b** Underground mine exposure of sub-vertical lenses of hematite-altered felsic porphyry in black tholeiitic mafic schist, and crosscutting, sub-horizontal, quartz–carbonate–chlorite veins with hematite-altered selvages (from Williams 1994). **c** Mineralised felsic porphyry (sample 121784, 3.65 g/t Au) and $\delta^{34}\text{S}_{(\text{py})}$ values. **d** Euhedral pyrite from the sample in c. **e** Weakly mineralised tholeiitic mafic schist (sample 121776, <0.01 g/t Au) and $\delta^{34}\text{S}_{(\text{py})}$ value. **f** Euhedral pyrite from the sample in e



values of ore-related pyrites in the regional study. However, there are some indicative relationships. First, there are indications that more negative $\delta^{34}\text{S}$ values correlate with higher gold grades, which is at least partly related to variations from proximal to distal alteration assemblages or proximity to veins. Second, there are variations related to contrasting host rocks, with rock with pre-existing magnetite and/or hematite alteration (e.g. New Celebration, Porphyry) showing more negative $\delta^{34}\text{S}$ values and greater ranges. Third, there are indications that structural style may be important. All of the deposits with mean negative $\delta^{34}\text{S}$ values from the regional dataset in Table 1 (Porphyry, New Celebration, Golden Mile) are hosted in brittle-ductile shear zones, whereas deposits dominated by vein arrays (e.g. Granny Smith, Mt Charlotte) have positive mean $\delta^{34}\text{S}$ values. Furthermore, there are indications that shear zone orientation may be important, with the gently dipping Porphyry deposit showing extreme variation in $\delta^{34}\text{S}$ values despite its small size, and the more negative $\delta^{34}\text{S}$ values from Sunrise Dam being from ore-related pyrites associated with the gently dipping Sunrise Shear Zone.

Deposit-scale study at Victory-Defiance

Introduction

Results from the regional study suggest that there are potential relationships between $\delta^{34}\text{S}_{(\text{py})}$, proximity to high-grade ore zones, host rock composition and structural style of mineralisation. Victory-Defiance was selected for a case study to test these relationships because it is a world-class deposit with a variety of host rocks and structural styles of mineralisation and with a large range of $\delta^{34}\text{S}_{(\text{py})}$ (Palin and Xu 2000).

The Victory-Defiance samples analysed in this study are those used for a lead isotope study of pyrites in the 32 Shear Zone. Ho et al. (1994) originally selected this zone because it has a range of mineralisation styles and host rocks, and mineralisation is interpreted to have occurred during a single structural event from a chemically homogeneous ore fluid (Clark et al. 1989). Analytical results from Ho et al. (1994) also include gold analyses of pyrite separates. The combination of data from this study and that of Ho et al. (1994) thus provides an opportunity to

Table 3 $\delta^{34}\text{S}$ values of ore-related pyrites (in order from most negative to most positive) and whole-rock gold values at New Celebration

Sample number	Sample description	$\delta^{34}\text{S}_{(\text{py})}$ ‰	Whole-rock Au (ppm)
121784	Mineralised felsic porphyry intrusion, albite–hematite alteration	−6.0, −8.6	3.7
121788	Mineralised tholeiitic mafic schist, alkali feldspar–albite–ankerite alteration	−5.5, −4.8	5.0
121763	Felsic porphyry intrusion, sericite alteration, 19.5 m from mineralised shear zone	−1.4	0.3
121766	Ultramafic schist, biotite–dolomite–chlorite alteration, 10 m below mineralised shear zone	+3.9	<0.01
121776	Tholeiitic mafic schist, chlorite–calcite–albite alteration, 39.5 m from mineralisation	+5.5	<0.01

Gold values from Williams (1994). $\delta^{34}\text{S}_{(\text{py})}$ values from this study

determine potential causes of variations in $\delta^{34}\text{S}_{(\text{py})}$ values in a world-class orogenic gold system.

Deposit geology

Victory-Defiance (Roberts and Elias 1990) is the second largest deposit, after the Golden Mile, along the Boulder-Lefroy Shear Zone, with pre-mining resources of over 250-t gold (Watchorn 1998). Gold mineralisation is hosted in brittle-ductile shear zones, quartz breccia zones and brittle quartz vein arrays (Fig. 8), in the Defiance Dolerite, Paringa Basalt and Kapai Slate; minor host rocks include the Flames Porphyry and Tripod Hill Komatiite (Clark et al. 1986). At the time of gold mineralisation, the principal compressional stress (σ_1) was sub-horizontal (Clark et al. 1986). Proximal alteration assemblages include quartz–albite–ankerite/dolomite–sericite–pyrite(–biotite) in basalt and dolerite, tremolite–biotite–talc–quartz–pyrite–dolomite in komatiite and quartz–albite–sericite–pyrite–ankerite (–magnetite–chlorite) in Kapai Slate and felsic intrusions (Clark et al. 1989). Geochronological studies (both U–Pb in rutile and Ar/Ar in sericite) constrain the timing of mineralisation to $2,627 \pm 14$ Ma (Clark 1987; Kent 1994). Fluid inclusion microthermometry and mineral equilibria (Clark et al. 1989) indicate a low to moderate salinity (8–9 wt.% NaCl equivalent), $\text{H}_2\text{O}-\text{CO}_2 \pm \text{CH}_4$ hydrothermal fluid, with P–T conditions of 170–200 MPa and 370–

390°C. A variety of different geochemical mechanisms for gold deposition have been proposed, including sulphidation reactions in iron-rich host rocks during fluid–rock interaction (Clark et al. 1989), phase separation and wall-rock carbonation (Palin and Xu 2000) and mixing of fluids with different redox states (Neumayr et al. 2005).

Distribution of sulphur isotopes

$\delta^{34}\text{S}_{(\text{py})}$ values at Victory-Defiance from this study are combined with those of Xu (1999) in Table 5. Samples analysed for this study are mainly from the gently dipping (15–30°) 32 Shear Zone ($n=22$), whereas samples analysed by Xu (1999; $n=20$) are from the southern and eastern parts of the deposit. By combining the results from these two studies into a more comprehensive dataset, the spatial distribution of variations in $\delta^{34}\text{S}_{(\text{py})}$ is more apparent. The average $\delta^{34}\text{S}_{(\text{py})}$ value from the combined dataset ($n=42$) is -2.3‰ (± 2.8), with a total range of -6.3‰ to $+5.1\text{‰}$.

Figure 8 shows the spatial distribution of gold-related $\delta^{34}\text{S}_{(\text{py})}$ values at Victory-Defiance in different structures. The most consistently negative $\delta^{34}\text{S}_{(\text{py})}$ values and the largest range of values (-6.3‰ to $+0.2\text{‰}$) are along the gently dipping Repulse Fault. More steeply dipping faults in the hanging wall of the Repulse Fault (Victoria, Britannia and Sirius Faults) have more positive $\delta^{34}\text{S}_{(\text{py})}$ values, ranging from -2.5‰ to $+2.7\text{‰}$. The largest range of

Fig. 6 Plot of whole-rock gold values vs pyrite $\delta^{34}\text{S}$ values from the New Celebration and Porphyry deposits, from the data in Tables 3 and 4

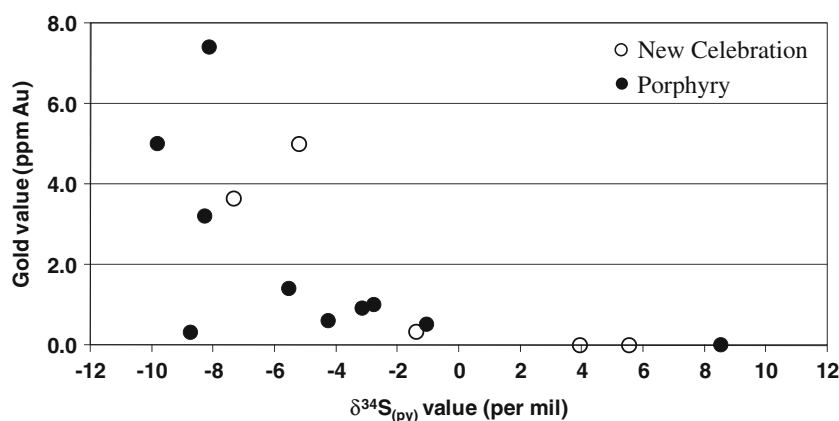
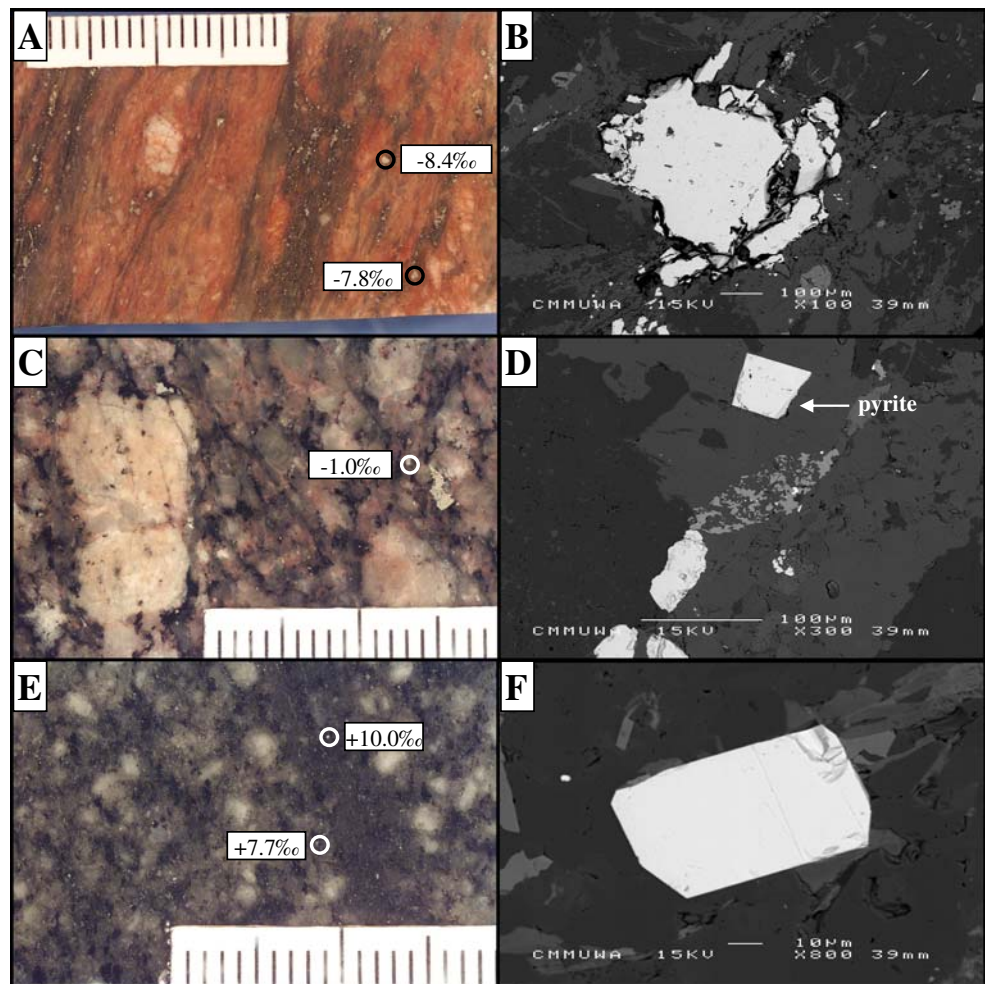


Fig. 7 Photographs and SEM images of quartz–monzonite host rock from the Porphyry deposit. *Scale bar* in photographs is in millimetre increments. **a** Well-mineralised sample (#101935, 7.4 g/t Au) with strong hematite alteration and well-developed shear fabric defined by pyrite and sericite. **b** Anhedral pyrite from the sample in **a**. **c** Weakly mineralised sample (#101958, 0.5 g/t Au) from shear zone margin, with weak hematite alteration and minor fabric development. **d** Euhedral pyrite from the sample in **c**. **e** Quartz monzonite (#101951, <0.01 g/t Au) with very weak fabric development, from approximately 10 m below the mineralised shear zone. **f** Small euhedral pyrite from the sample in **e**



$\delta^{34}\text{S}_{(\text{py})}$ values is in the 31, 32 and 33 Shear Zones, which are gently dipping structures in the footwall of the Repulse Fault, and includes $\delta^{34}\text{S}$ values ranging from -4.4% to $+5.1\%$. There are no significant relationships between $\delta^{34}\text{S}_{(\text{py})}$ values and host rock types (Table 5).

Sulphur isotopes and gold grades

There is a broad negative correlation between gold values of pyrite separates and pyrite $\delta^{34}\text{S}$ values at Victory-Defiance (Fig. 9 and Table 5). Palin and Xu (2000)

Table 4 $\delta^{34}\text{S}$ values of ore-related pyrites (in order from most negative to most positive) and whole-rock gold values, in quartz–monzonite host rocks at Porphyry

Sample number	Sample description	$\delta^{34}\text{S}_{(\text{py})}$ ‰	Whole-rock Au (ppm)
101956	Sheared quartz monzonite, strong hematite alteration, visible gold	-10.2, -9.4	5.0
101929	Sheared quartz monzonite, moderate hematite alteration	-9.7, -7.7	0.3
101935	Sheared quartz monzonite, strong hematite alteration, visible gold	-8.4, -7.8	7.4
101987	Sheared quartz monzonite, strong hematite alteration	-8.3	3.2
101984	Sheared quartz monzonite, weak hematite alteration	-5.6	1.4
101990	Quartz monzonite, weak hematite alteration	-4.3	0.6
101955	Sheared quartz monzonite, moderate hematite alteration	-2.8	1.0
101931	Sheared quartz monzonite, strong hematite alteration	-2.2, -4.1	0.9
101958	Sheared quartz monzonite, weak hematite alteration	-1.0	0.5
101951	Grey quartz monzonite, 10 m below shear zone	+10.0, +7.1	<0.01

Gold values from Allen (1986). $\delta^{34}\text{S}_{(\text{py})}$ values from this study.

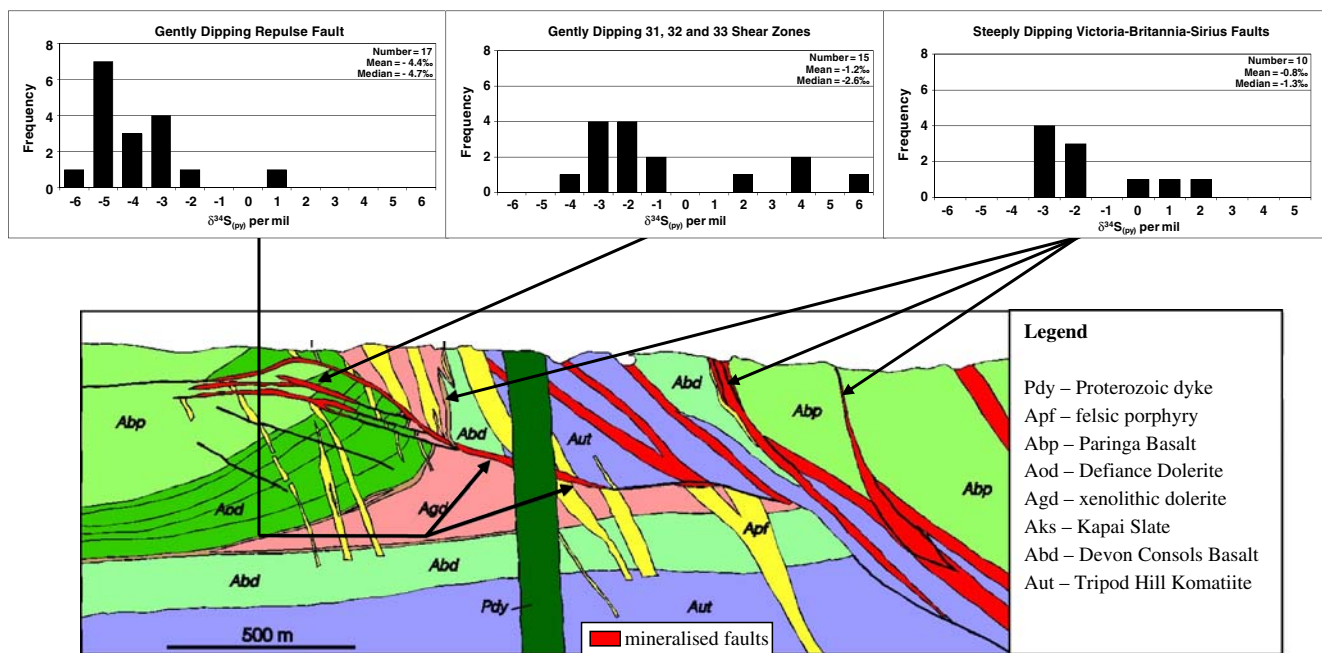


Fig. 8 Cross section of the Victory-Defiance area, view to the northwest (modified from Vanderhor and Groves 1998), showing average $\delta^{34}\text{S}_{(\text{py})}$ values and ranges in different structures (data from Table 5). Sub-horizontal shortening during gold mineralisation (Clark

et al. 1986; Vearncombe et al. 1989) would cause dilation in gently dipping faults and compression or transpression in steeply dipping faults

document a similar negative correlation between whole-rock gold values, from core and mine samples, and pyrite $\delta^{34}\text{S}$ values. We have shown similar relationships between whole-rock gold values and pyrite $\delta^{34}\text{S}$ values at New Celebration and Porphyry (Fig. 6).

Summary of sulphur isotope data

The following trends are apparent in the combined new and existing $\delta^{34}\text{S}$ data from the Eastern Goldfields Province.

1. The $\delta^{34}\text{S}$ values have a total range from about -10‰ to $+12\text{‰}$, with considerable overlap between sulphides from different deposits between -4‰ and $+4\text{‰}$, centred on 0‰ (Fig. 3).
2. Most deposits have gold-related pyrites with mean $\delta^{34}\text{S}$ values between 0‰ and $+4\text{‰}$ with a relatively restricted range of values, normally less than 8‰ if obvious outliers are excluded (Fig. 3). However, other deposits have mean $\delta^{34}\text{S}$ values between -2‰ and -4‰ , commonly with far greater ranges in $\delta^{34}\text{S}$ values (Fig. 3), normally greater than 10‰ and potentially in excess of 22‰ (e.g. Golden Mile: Fig. 3).
3. There is no obvious consistent geographic relationship between gold deposits in the two groups (Fig. 2). Three of the deposits with negative means and large ranges of

$\delta^{34}\text{S}$, Golden Mile, New Celebration and Victory-Defiance, occur in the southern part of the Kalgoorlie Terrane (Fig. 2) adjacent to the Boulder-Lefroy Shear Zone. However, Mt. Charlotte, which is sited adjacent to the Golden Mile, and Hunt and Junction, which are close to Victory-Defiance, fall into the groups with positive mean $\delta^{34}\text{S}$ values and limited ranges of isotope ratios (Fig. 3).

4. In each of the three deposits studied that have large ranges and low mean $\delta^{34}\text{S}$ (New Celebration, Porphyry, Victory-Defiance), the highest gold grades are associated with low $\delta^{34}\text{S}$ values (Figs. 6 and 9). There is no consistent relationship between the mean and total range of $\delta^{34}\text{S}$ values of a deposit and its size, although several of the larger deposits as well as the small Porphyry deposit have large ranges in $\delta^{34}\text{S}$ (Table 2).
5. Importantly, there is a potentially better fit between the structural style of deposit and range of $\delta^{34}\text{S}$ values (Table 2). There is a strong tendency for shear-zone-hosted deposits to have a greater range of $\delta^{34}\text{S}$ values than stockwork, vein-hosted or disseminated deposits. Pre-existing hematite or magnetite alteration also appears to favour the deposition of pyrites with negative $\delta^{34}\text{S}$ values in some deposits (e.g. New Celebration; Fig. 5a).
6. Most importantly, the study at Victory-Defiance also suggests that, with a sub-horizontal σ_1 , the more dilational, more gently dipping shear zones have more

Table 5 $\delta^{34}\text{S}$ values from Victory-Defiance ore-related pyrites, from this study and Xu (1999)

Sample number	Host rock	$\delta^{34}\text{S}_{(\text{py})}$ ‰	Host structure	Au (ppm)	Data sources
104360BA	Flames Porphyry	-3.9	Repulse Fault	1	Ho et al. (1994); this study
104358ACi	Flames Porphyry	-3.7	Repulse Fault	16	Ho et al. (1994); this study
104361A	Flames Porphyry	-3.9	Repulse Fault	45	Ho et al. (1994); this study
104357AA	Flames Porphyry	-4.7	Repulse Fault	16	Ho et al. (1994); this study
VO15	Flames Porphyry	-2.3	Repulse Fault		Xu (1999)
104350BB	Flames Porphyry	-2.2	Victory Fault	85	Ho et al. (1994); this study
104350BE	Flames Porphyry	-2.1	Victory Fault	189	Ho et al. (1994); this study
104350A	Flames Porphyry	-2.0	Victory Fault	161	Ho et al. (1994); this study
CD2193, 274.6 m	Paringa Basalt	-2.0	32 Shear zone		Xu (1999)
104364CAi	Paringa Basalt	-3.6	32 Shear zone	9	Ho et al. (1994); this study
VU4-13, 120.75 m	Paringa Basalt	3.3	32 Shear zone		Xu (1999)
VO40	Paringa Basalt	2.0	Sirius Fault		Xu (1999)
CD2193, 87.3 m	Paringa Basalt	-3.5	31 Shear zone		Xu (1999)
CD2231, 171.7 m	Paringa Basalt	-2.6	32 Shear zone		Xu (1999)
VO01	Paringa Basalt	-4.4	32 Shear zone		Xu (1999)
104366BE	Paringa Basalt	-3.0	Repulse Fault	590	Ho et al. (1994); this study
104362AA	Paringa Basalt	-4.4	Repulse Fault	398	Ho et al. (1994); this study
VU4-4, 62.75 m	Defiance Dolerite	5.1	32 Shear zone		Xu (1999)
VU4-4, 73.3 m	Defiance Dolerite	3.5	32 Shear zone		Xu (1999)
CD2423, 389.5 m	Defiance Dolerite	-3.0	32 Shear zone		Xu (1999)
VO13	Defiance Dolerite	-1.6	32 Shear zone		Xu (1999)
VO16	Defiance Dolerite	-1.8	33 Shear zone		Xu (1999)
VO34	Defiance Dolerite	-2.7	33 Shear zone		Xu (1999)
VU4-10, 71.5m	Defiance Dolerite	1.1	32 Shear zone		Xu (1999)
VU4-4, 38.2 m	Defiance Dolerite	-3.1	31 Shear zone		Xu (1999)
104370ACi	Defiance Dolerite	-5.8	Repulse Fault	123	Ho et al. (1994); this study
104369BE	Defiance Dolerite	-5.0	Repulse Fault	252	Ho et al. (1994); this study
104354AC	Defiance Dolerite	-5.2	Repulse Fault	451	Ho et al. (1994); this study
104354BD	Defiance Dolerite	-5.8	Repulse Fault	187	Ho et al. (1994); this study
104352CF	Kapai Slate	-1.2	Victory Fault	5	Ho et al. (1994); this study
VO27	Kapai Slate	-1.0	Britannia Fault		Xu (1999)
VO49	Kapai Slate	0.2	Britannia Fault		Xu (1999)
VO50	Kapai Slate	2.7	Britannia Fault		Xu (1999)
104352A	Kapai Slate	-1.5	Victory Fault	46	Ho et al. (1994); this study
104352DB	Kapai Slate	-2.5	Victory Fault	85	Ho et al. (1994); this study
104367EQC	Devon Consols Basalt	-2.7	32 Shear zone	36	Ho et al. (1994); this study
104355AC	Devon Consols Basalt	-5.6	Repulse Fault	88	Ho et al. (1994); this study
104355BD	Devon Consols Basalt	-6.3	Repulse Fault	262	Ho et al. (1994); this study
104373AD	Tripod Hill Komatiite	-4.4	Repulse Fault	24	Ho et al. (1994); this study
104372AD	Tripod Hill Komatiite	-5.3	Repulse Fault	27	Ho et al. (1994); this study
104371BE	Tripod Hill Komatiite	-5.1	Repulse Fault	43	Ho et al. (1994); this study
CD4997, 237.45 m	Tripod Hill Komatiite	0.2	Repulse Fault		Xu (1999)

Samples listed in lithostratigraphic order of host rocks (see Fig. 8). Au part-per-million values of pyrite separates are from Ho et al. (1994). Sample numbers are from respective studies. Host structures are shown in Fig. 8

negative mean $\delta^{34}\text{S}$ values and a larger range of $\delta^{34}\text{S}$ than structures oriented such that they were compressional during gold mineralisation (Fig. 8). In this respect, it is interesting that the gently dipping Porphyry shear zone hosts pyrites with the greatest range of $\delta^{34}\text{S}$ values outside the Golden Mile and that the gently dipping Sunrise Shear Zone hosts ore-related

pyrites with the most negative $\delta^{34}\text{S}$ values at Sunrise Dam.

- Large variations in $\delta^{34}\text{S}$ values can occur on the centimetre-to-millimetre scale, with adjacent pyrites having markedly contrasting $\delta^{34}\text{S}$ values (e.g. Fig. 4c,f). This suggests very local controls on fluid oxidation state and consequent $\delta^{34}\text{S}$ values.

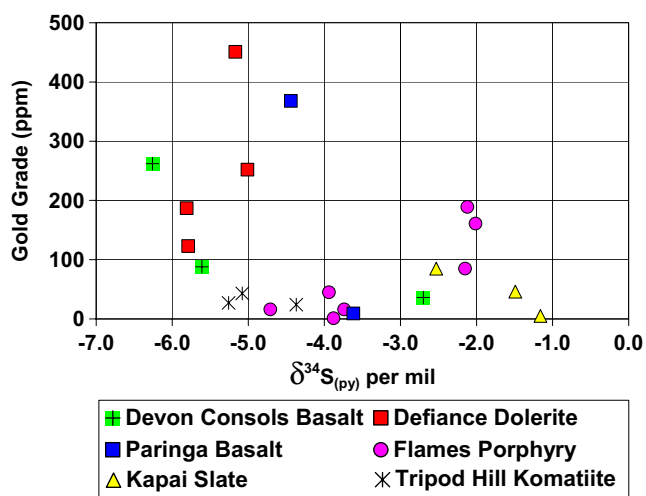


Fig. 9 Plot of gold value and $\delta^{34}\text{S}$ from Victory-Defiance ore-related pyrites, showing broad correlation between higher gold grades and more negative $\delta^{34}\text{S}$. Data are from this study and Ho et al. (1994) as shown in Table 5

Discussion

Introduction

The average $\delta^{34}\text{S}$ values of potential Archean sulphur reservoirs (i.e. pre-existing sulphides in host rocks, dissolved sulphate in seawater and sulphur-bearing magmatic volatiles) overlap between approximately 0‰ and +10‰ (Donnelly et al. 1978; Ohmoto and Rye 1979; Seccombe et al. 1981; Lambert et al. 1984; Ohmoto and Goldhaber 1997). This range of positive $\delta^{34}\text{S}$ values cannot directly account for the negative $\delta^{34}\text{S}_{(\text{py})}$ values of pyrites that occur in some orogenic gold deposits. Rather, these require variable proportions of oxidised and reduced sulphur species in the ore fluid. The various processes that could produce such variations are discussed below.

Magmatic source

A potential source of oxidised sulphur species is felsic intrusions (Cameron and Hattori 1987). However, such oxidised solutions would have to remain internally buffered during transport and gold precipitation. Ridley and Diamond (2000) suggest that orogenic ore-fluid compositions are unlikely to reflect the fluid source, given implied fluid travel distances, but rather reflect the influence of fluid–rock interactions along fluid pathways and ore-depositional processes at the deposit site. More importantly, there is no published evidence for any volumetrically significant coeval igneous rocks in the Eastern Goldfields Province that could have supplied oxidised magmatic–hydrothermal fluids (e.g. Witt and Vanderhor 1998; Hagemann and Cassidy 2000). The only precisely dated igneous rocks that

are within error of the age of robustly dated (SHRIMP in hydrothermal phosphates) gold mineralisation are volumetrically minor lamprophyres and hornblende-phyric dykes in the Kalgoorlie gold camp (McNaughton et al. 2006; Vielreicher et al. 2007) in which there are no exposed intrusions of significant size. Where detailed geochronological studies have been carried out (Salier et al. 2005), the orogenic gold deposits are significantly younger than intrusions of the high-Ca, mafic and alkaline suites of Champion and Cassidy (2002), which are those most likely to have produced oxidised fluids. These results support the view that Archean orogenic ore fluids were initially reduced and, under certain conditions, became oxidised along some pathways or at some depositional sites (Lambert et al. 1984; Phillips et al. 1986; Golding et al. 1990; Evans et al. 2006). In addition, the correlation between high gold values and negative $\delta^{34}\text{S}$ values in ore-related pyrites at Porphyry, New Celebration and Victory-Defiance, as shown in this study, suggests that whatever process caused oxidation of the primary ore fluid and formation of ore-related pyrites with negative $\delta^{34}\text{S}$ values in some deposits also played a potentially important role in gold precipitation (cf. Palin and Xu 2000). Ore-depositional processes that can potentially cause oxidation of orogenic ore fluids are discussed below, in relation to specific deposits analysed in this study.

Mixing with magmatic fluid

Although Mikucki (1998) considered that fluid mixing was not an important gold-depositing process, except at very high crustal levels, fluid-mixing models (e.g. Walshe et al. 1999; Hall et al. 2001; Neumayr et al. 2005) have recently been proposed for Yilgarn orogenic gold systems, based on distributions of oxidised and reduced alteration mineral assemblages. The models invoke mixing between a ubiquitous, deeply derived, relatively reduced fluid from a distal source and a more proximal, locally oxidising magmatic fluid.

Mixing of oxidised and reduced fluids contemporaneously in the same or adjacent fault zones, even though well established for epithermal gold deposits (Henly and Ellis 1983), is presently not supported by fluid inclusion nor stable-isotope datasets (Hagemann and Cassidy 2000). In addition, as discussed above, there are currently no geochronological data available that support formation of oxidised granites that are contemporaneous with reduced fluids that form orogenic gold deposits. There is a case for gold mineralisation that broadly overlaps with the initiation of crustal melting and emplacement of the low-Ca granite suite of Champion and Cassidy (2002), as shown, for example, by Qui and McNaughton (1999) and Salier et al. (2005). However, these granitoids are generally reduced, not oxidised.

Reaction with pre-existing oxidised alteration assemblages

This type of process has recently been proposed by Neumayr et al. (2005) for the St. Ives gold camp. A significant change in the redox state of the hydrothermal fluids during gold mineralisation is interpreted to be due to reaction between a ubiquitous, deeply derived reduced ore fluid and the products of reactions (e.g. hematite or magnetite) between reduced amphibolite host rocks and oxidised fluids released from granitoids underneath and within the greenstone belt rocks. This early magmatic alteration of reduced basalts and subsequent reduced hydrothermal fluid flow in the same fault corridor is also described by Kenworthy and Hagemann (2005) for the Darlot gold deposits. Whether such early oxidised alteration assemblages are part of the orogenic gold event or related to a completely separate earlier event has not been resolved, although available geochronology supports the latter reason (e.g. Salier et al. 2005). It may also not be necessary for the oxidised alteration assemblages to be related to magmatic processes (cf. Huston et al. 2001). Whatever the timing, such reactions between reduced ore fluid and earlier alteration is supported, for example, at New Celebration where ore-related pyrites with negative $\delta^{34}\text{S}$ values occur predominantly in two host rock types: mafic schist, with ubiquitous pre-gold magnetite alteration, and felsic porphyry dykes, with abundant pre-gold hematite alteration. The most likely explanation is that the interaction of the primary ore fluid with these Fe^{3+} -rich rocks resulted in ore-fluid oxidation at, or near, the site of gold deposition, which, in turn, resulted in deposition of sulphides with negative $\delta^{34}\text{S}$ values. A potential analogy is the Archean orogenic gold Francoeur 3 deposit in Quebec, which has negative $\delta^{34}\text{S}$ values in gold-related pyrite. Couture and Pilote (1993) interpreted gold mineralisation at Francoeur 3 to be the result of fluid–rock interaction and progressive changes in ore-fluid oxidation state, associated, in part, with reaction of the orogenic ore fluid with pre-gold hematite alteration.

Mixing of two modified fluids from a single source

In a detailed study of orogenic ore-fluid evolution in the Yilgarn Golden Crown deposit, Uemoto et al. (2002) show that gold mineralisation is associated with mixing between two modified components of a single orogenic ore fluid. In this genetic model, an $\text{H}_2\text{O}-\text{CO}_2$ ore fluid from a single source is interpreted to have migrated upwards along a shear zone. In the northern end of the deposit, the fluid reacted with graphitic shale and became a relatively reduced $\text{H}_2\text{O}-\text{CO}_2 \pm \text{CH}_4$ fluid. The addition of CH_4 , from reaction with the shale, raised the solvus to higher P–T conditions and, in combination with a local decrease in fluid pressure due to fracture opening, enhanced phase

separation and gold precipitation. In addition, reaction with the graphitic shale could have caused a decrease in $a\text{H}_2\text{S}_{(\text{aq})}$, accounting for somewhat higher gold grades at the shale contact. In other parts of the deposit, the primary ore fluid reacted with dolerite and became a relatively oxidised $\text{H}_2\text{O}-\text{CO}_2$ fluid. Mixing of the two evolved ore-fluid components in the upper parts of the deposit is interpreted to have oxidised the reduced ore fluid and promoted gold precipitation in the mixing zone.

Although this type of fluid mixing has not been documented for any of the deposits investigated in this study (see Table 2), it could account for the occurrence of distinct oxidised and reduced fluids in the same orogenic gold system, as the result of interaction of a typical orogenic ore fluid with variably reduced and oxidised rocks in the host rock sequence. However, it is unlikely to have resulted in sufficiently oxidised fluids to cause the highly negative $\delta^{34}\text{S}_{(\text{py})}$ shifts elsewhere as magnetite, not hematite, is stable in the metamorphic assemblage and pyrrhotite, pyrite and arsenopyrite are stable in the muscovite alteration zone.

Reactions with host rocks

Orogenic fluids in the Yilgarn craton are thought to have been broadly controlled by sulphate–sulphide or by carbonate–methane fluid buffers, depending upon the temperature and initial composition (Mikucki and Ridley 1993). However, the high oxidation states deduced for some gold-deposit fluids require mechanisms to depart from regional fluid buffers. From the example of Uemoto et al. (2002), it is evident that wall-rock reactions can modify the oxidation state of the ore fluid. Also, sulphidation of Fe-bearing minerals (e.g. Phillips and Groves 1983) is widely accepted as a major gold-depositional process and sulphidation of Fe oxides has been suggested as a mechanism to raise the oxidation state of ore fluids (e.g. Phillips et al. 1986; Evans et al. 2006). The association of negative $\delta^{34}\text{S}$ values with pre-existing Fe-oxide alteration at deposits such as Porphyry demonstrates that this is a plausible oxidation mechanism, but the fact that pyrites from deposits clearly formed by sulphidation of Fe oxides (e.g. Mt Charlotte, Water Tank Hill, Wallaby) do not necessarily have negative $\delta^{34}\text{S}$ values requires that it cannot be a universal mechanism.

A more universal wall-rock reaction is carbonation because the ore fluid is ubiquitously CO_2 rich. During wall-rock carbonation, the reaction of CO_2 -bearing hydrothermal fluids with ferric-iron-bearing minerals (e.g. magnetite) forms Fe-bearing carbonates, characteristic of orogenic gold deposits (McCuaig and Kerrich 1998). This reaction can result in significant oxidation of the ore fluid (Palin and Xu 2000; Palin et al. 2001), leading to negative shifts in $\delta^{34}\text{S}$ of H_2S , as the proportion of HSO_4 to H_2S in the solution increases, with resultant negative $\delta^{34}\text{S}$ values

in gold-related pyrite. Thus, it is possible that, under certain conditions, orogenic ore fluids become oxidised as a result of carbonation reactions, rather than sulphidation, with Fe oxides in wall rocks (Phillips et al. 1986, 1996). This process can explain the negative $\delta^{34}\text{S}$ values in ore-related pyrites in magnetite-rich mafic host rocks at Victory-Defiance and New Celebration, but they are lacking in other rocks exceedingly rich in magnetite (e.g. BIF) where elements such as Ca and Mg may be too low for effective stabilisation of abundant ore-related carbonates.

Phase separation

Phase separation offers another avenue for departure from fluid buffers, resulting in oxidation of fluids (Rye 1993). In all Yilgarn deposits that have received detailed fluid inclusion study, there is evidence for phase separation in ore fluids (Table 2). During phase separation, reduced gases, such as H_2 , CH_4 and H_2S , are preferentially partitioned into a vapour phase, which increases the ratio of SO_4 to H_2S in the residual ore fluid, leaving it relatively oxidised (Drummond and Ohmoto 1985). Under equilibrium conditions, phase separation leads to relatively ^{34}S -depleted H_2S in the residual ore fluid and results in the precipitation of sulphide minerals with more negative $\delta^{34}\text{S}$ values (Ohmoto and Rye 1979; Ohmoto 1986). Removal of H_2S from the ore fluid into the vapour phase during phase separation also causes a decrease in the total activity of sulphur ($a\Sigma\text{S}$) in gold ore fluids, which destabilises gold-bisulphide complexes and shifts the fluid from the pyrite stability field to the pyrite-hematite equilibrium curve (Fig. 10). This results in a rapid decrease in gold solubility and the precipitation of pyrite in equilibrium with hematite. Therefore, rapid pressure changes and associated phase separation are potentially efficient mechanisms for ore-fluid oxidation and hence gold deposition. Cassidy (1992) and Witt (1995) suggest phase separation as the main cause of gold deposition and hematite alteration in orogenic gold deposits in low-Fe host rocks. This process can explain the occurrence of gold mineralisation at Porphyry and the wide range of $\delta^{34}\text{S}$ values of ore-related pyrites within it.

At Sunrise Dam, there is evidence for intermittent phase separation in fluid inclusions from the Sunrise Shear Zone (Brown 2002). Phase separation is interpreted to be related to hydraulic fracturing associated with competency contrasts between felsic volcanoclastic sedimentary rocks and more brittle magnetite-rich shale units (Brown 2002). The occurrence of the shale units as thin beds within the host rock sequence suggests that fracturing related to competency contrasts and associated phase separation may have occurred only locally. This would account for the rare occurrences of negative $\delta^{34}\text{S}$ values (one of seven samples from the Sunrise Shear Zone). The average $\delta^{34}\text{S}$ value in

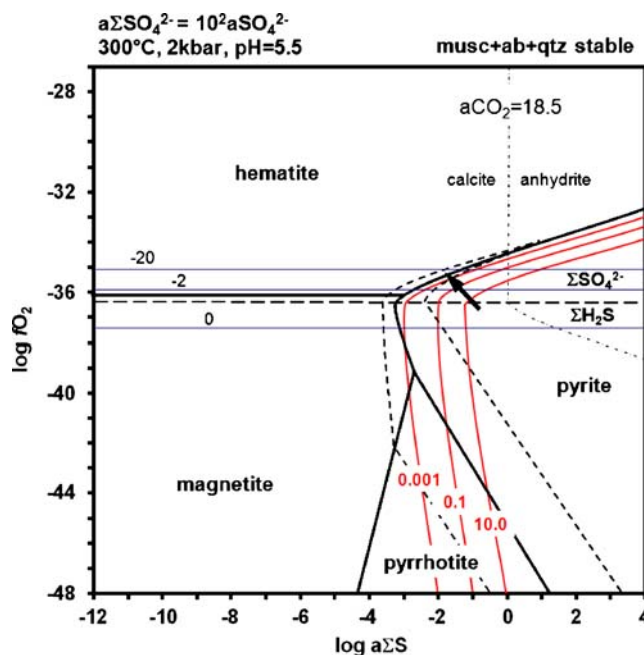


Fig. 10 Plot of oxygen fugacity ($\log f\text{O}_2$) and activity of total sulphur ($a\Sigma\text{S}$), showing gold-solubility contours (0.001, 0.1 and 10.0 ppm) for gold-bisulphide complexes, modified from Mikucki and Groves (1990). During phase separation in a reduced ore fluid, reduced gases such as H_2S , CH_4 and H_2 are preferentially partitioned into a vapour phase, which reduces $a\Sigma\text{S}$ and leaves a relatively oxidised ore fluid (Drummond and Ohmoto 1985). The resulting shift from the pyrite stability field to the pyrite-hematite equilibrium curve destabilises the gold-bisulphide complex and causes a significant decrease in gold solubility (see arrow across the steep gold-solubility gradient). In this case, gold mineralisation would be accompanied by increased hematite alteration. Isotopic contours are drawn as H_2S values. They were drawn with the aid of Zhang and Spry (1994), assuming, $m\text{Na}^+ = 1$, $m\text{K}^+ = 0.1$ and $m\text{Ca}^{2+} = 0.01$ and total $\delta^{34}\text{S} = 0\text{‰}$

gold-related pyrites at Sunrise Dam is $+1.1\text{‰}$ (± 3.5) consistent with the dominant gold-depositional mechanism interpreted to be wall-rock sulphidation (Brown 2002).

Phase separation has also been interpreted as a potential gold-depositional mechanism at Lady Bountiful and North Royal. Based on analytical results from this study, there are rare occurrences of ore-related pyrites with more positive $\delta^{34}\text{S}$ values in these two deposits. In a detailed study of the Mt. Charlotte deposit, Harbi (1997) provides evidence for phase separation under both equilibrium and disequilibrium conditions, in different parts of the hydrothermal system. During phase separation under disequilibrium conditions, H_2S in the residual ore fluid becomes relatively enriched in ^{34}S , which results in the formation of sulphide minerals with more positive $\delta^{34}\text{S}$ values (Ohmoto and Rye 1979).

At Victory-Defiance, the large range of $\delta^{34}\text{S}$ values in ore-related pyrites and a negative correlation between $\delta^{34}\text{S}_{(\text{py})}$ values and gold grade in mafic host rocks (Fig. 9) indicate an increase in fluid oxidation during mineralisation. Previous studies at Victory-Defiance (Clark et al. 1989) show that wall-rock sulphidation is a significant ore-

forming process. However, this process alone cannot produce the degree of fluid oxidation necessary to explain the range in sulphur isotopes (Mikucki and Groves 1990). Based on fluid–rock reaction path calculations (Palin and Xu 2000; Palin et al. 2001), the two dominant in situ mechanisms that potentially caused oxidation of originally reduced ore fluids at Victory-Defiance were carbonation of wall-rock magnetite and phase separation.

Structural style: rock-dominated vs fluid-dominated systems

There is a strong tendency for deposits hosted in brittle-ductile shear zones to have greater ranges and more negative mean $\delta^{34}\text{S}$ values than stockwork, vein-hosted or disseminated mineralisation (Fig. 11); for example, eight of the 11 deposits with $\delta^{34}\text{S}$ ranges of 10‰ or more are hosted in shear zones. While it must be remembered that the ranges are based on different population sizes, it is important that the relationship with structural style is stronger than that with deposit size or any other single factor considered in this study.

As a specific well-documented example, the structural setting at Victory-Defiance appears to have been a critical factor in controlling the distribution of $\delta^{34}\text{S}$ values of ore-related pyrites. As discussed above, large fluid-pressure fluctuations can lead to oxidation of ore fluids and cause gold deposition. At Victory-Defiance, pyrites with negative $\delta^{34}\text{S}$ values occur in gently dipping structures whereas those with more positive $\delta^{34}\text{S}_{(\text{py})}$ values occur in steeply dipping structures (Fig. 8). This suggests a potential relationship between the $\delta^{34}\text{S}$ value of ore-related pyrites, structures and fluid-pressure fluctuations during fault-valve

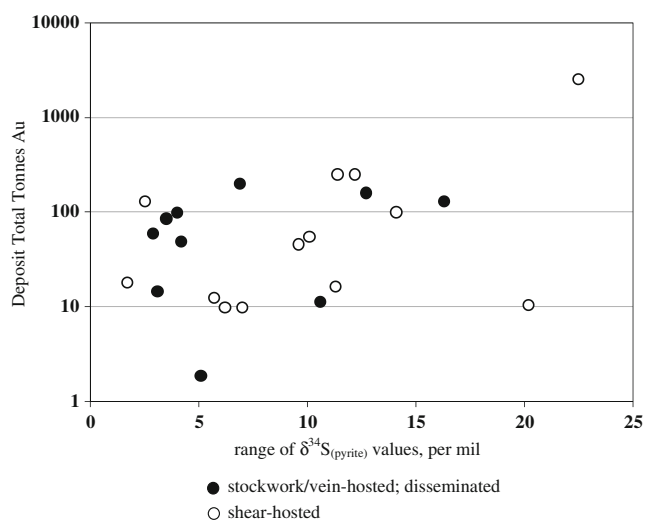


Fig. 11 Plot showing broad relationship between gold endowment and total range of $\delta^{34}\text{S}_{(\text{py})}$ values, by dominant structural style of mineralisation, from deposits in Table 1 with more than one sample

cycles. These cycles are controlled by the progressive buildup of fluid pressures between rupture events in fault systems that localise fluid flow (Sibson et al. 1988). Structural analysis and fluid inclusion studies in the Val d'Or district (Robert et al. 1995) indicate large fluid-pressure fluctuations in laminated and extensional veins during mineralisation. Other studies use fluid inclusion evidence for phase separation to link large fluid-pressure fluctuations to gold deposition in high-grade (>10 g/t) veins at the Pamour, Hollinger-McIntyre and Sigma deposits (Walsh et al. 1988; Guha et al. 1991). During sub-horizontal shortening (Clark et al. 1986; Vearncombe et al. 1989), the gently dipping structures at Victory-Defiance would be in the optimal orientation for dilation and focussed fluid flow during faulting, whereas the steeply dipping structures would be sites of compression or transpression, with more transient fluid flow. This relationship suggests that different fluid-flow regimes in broadly dilational and compressional structures influence physical and chemical conditions in the ore fluid and hence $\delta^{34}\text{S}$ values in gold-related pyrites.

At the Revenge deposit, located 5 km northwest of Victory-Defiance, Nguyen et al. (1998) demonstrate that fault-valve activity influenced the formation of optimally oriented, gently dipping, shear zones in a transitional brittle-ductile regime. Large fluid-pressure fluctuations are interpreted to have controlled the localisation of fluid flow and associated gold mineralisation along active shear zones. At Revenge, there are also relationships between $\delta^{13}\text{C}$ of gold-related carbonate minerals and orientations of mineralisation-hosting structures (Nguyen 1997). This again suggests that different fluid-flow regimes in different structures can influence the isotopic signature of ore fluids within them.

The degree of dilatancy of ore-hosting structures probably reflects the degree to which fluid-dominated or rock-buffered processes acted. In dilatant shear zones, internal fluid-dominated processes, such as phase separation, caused pulsed variations in oxidation state. However, in less-dilatant structures, the fluids fractured the rock by processes such as crack seal or hydraulic fracturing such that continuous reactions with wall rocks led to largely rock-buffered systems.

Summary

Based on the discussion above, variations in $\delta^{34}\text{S}$ values of ore-related pyrites can be caused by the inferred dominant ore-depositional processes in orogenic gold systems: fluid–rock interaction, phase separation and mixing of modified fluids from a single source. In the seismogenic regime, fluid-pressure fluctuations and consequent reversals in pressure gradients influence the operation of these processes and cause episodic gold deposition at different stages in

the seismic cycle (Cox 1999). For example, pre-failure fluid discharge from faults enhances fluid–rock interaction in host rocks adjacent to faults, while fluid pressures increase beneath low-permeability seals that cap the hydrothermal system. At this stage of the seismic cycle, wall-rock sulphidation reactions in iron-rich host rocks may generate disseminated gold mineralisation under rock-buffered conditions. In addition, wall-rock carbonation of Fe³⁺-rich host rocks (e.g. magnetite-rich dolerite at the Golden Mile, New Celebration and Victory-Defiance) could cause oxidation of orogenic gold fluids (Phillips et al. 1986; Palin and Xu 2000; Evans et al. 2006) during this pre-failure stage.

During and immediately after faulting in the seismic cycle, rapid fluid-pressure fluctuations can cause phase separation, resulting in both ore-fluid oxidation and gold precipitation, as discussed above. Pressure fluctuations are most severe at dilational sites, and, importantly, results from this study suggest that the larger variations in $\delta^{34}\text{S}$ values are commonly associated with more dilational structures in the ore environment where internal fluid-dominated processes may be dominant.

In the immediate post-failure stage of the seismic cycle, fluid mixing between primary ore fluids and modified equivalents, which have reacted with wall rocks, may cause oxidation and gold deposition. During the pre-failure discharge of fluids from faults, reactions between the primary ore fluid and variably reduced or oxidised wall rocks (e.g. graphitic shale or dolerite; Uemoto et al. 2002) can change the oxidation state of the ore fluid. During shear failure and dilation, pressure changes cause these modified ore fluids to be drawn back into faults which are pathways for the primary ore fluid. Subsequent back-mixing between the two fluids will result in gold deposition.

It is evident that a variety of processes, all of which are described from detailed research on one or more Yilgarn deposits, can explain the highly oxidised nature of some Archean orogenic gold deposits, without appeal to exotic fluid sources, such as those derived from magmatic systems (cf. Walshe et al. 1999; Hall et al. 2001).

Sulphur isotopes and gold endowment

A plot of gold endowment and total variation in $\delta^{34}\text{S}_{(\text{py})}$ values (Fig. 11) show that many larger orogenic gold deposits (>30 t Au) have larger ranges of $\delta^{34}\text{S}_{(\text{py})}$ values (greater than approximately 10‰), although this is not a consistent relationship. This broad relationship is potentially an indication of the influence of multiple ore-forming processes (e.g. wall-rock sulphidation, wall-rock carbonation and phase separation) in complex ore systems at deposits such as Victory-Defiance and the Golden Mile, as discussed above. Large ranges of $\delta^{34}\text{S}_{(\text{py})}$ values in smaller deposits may indicate the influence of a single dominant

ore-depositional process (e.g. phase separation at Porphyry). Most of the larger deposits with large ranges of $\delta^{34}\text{S}_{(\text{py})}$ values are dominantly shear-zone-hosted, rather than stock-work, vein-hosted or disseminated, suggesting that multiple ore-forming processes are more likely to occur in mineralising systems where larger fluid volumes circulated through more-continuous structural permeability paths and where fluid-dominated systems, rather than rock-buffered systems, were predominant.

The determination of $\delta^{34}\text{S}$ values in sulphide minerals requires a detailed sample preparation and analysis, which is well beyond the scope of most exploration programmes. However, multiple ore-depositional processes at a single deposit location are potentially critical factors for large gold endowment and high gold grade. Therefore, the recognition of more than one potential gold-precipitation mechanism in an orogenic gold system is important. Analysis of $\delta^{34}\text{S}$ values in sulphides would complement structural, alteration and fluid inclusion studies that similarly seek to identify multiple ore-forming processes. Sulphur isotopic compositions alone cannot uniquely define potential endowment, as shown by the fact that the Porphyry deposit has an extreme range in $\delta^{34}\text{S}_{(\text{py})}$ values but is quite small.

Conclusions

Based on the results of this and previous studies, there is abundant evidence for in situ oxidation of orogenic ore fluids associated with different gold-depositional processes. Phase separation and fluid–rock interaction are the most common processes recorded by a variety of researchers for deposits examined in this study. The former fluid-dominated process appears to produce greater shifts in fluid oxidation state. Mixing of two modified components of a single ore fluid is also an effective process of oxidation and gold deposition (Uemoto et al. 2002), although this mechanism is not documented by any author for the deposits studied here. Similarly, only fluid inclusion studies from deposits at high crustal levels (e.g. Wiluna, Hagemann 1992; Racetrack, Gebre-Mariam 1994) suggest mixing of external fluids in orogenic gold systems in the Eastern Goldfields Province.

The influence of more than one gold-depositional mechanism during the formation of a single deposit has the potential to increase gold endowment. Therefore, the recognition of multiple gold-depositional processes is significant in the study of, and exploration for, world-class orogenic gold deposits. Analysis of $\delta^{34}\text{S}_{(\text{py})}$ provides one method for recognising the influence of multiple ore-forming processes.

The structural setting of a deposit is potentially the most important factor controlling ore-fluid oxidation and hence the distribution of $\delta^{34}\text{S}_{(\text{py})}$ values. At Victory-Defiance, pyrites

with negative $\delta^{34}\text{S}$ values occur more commonly in gently dipping dilational structures, compared to steeply dipping structures. In this study, it is proposed that these differences are associated with fluid-pressure fluctuations during fault-valve cycles, which establish different fluid-flow regimes in structures with different orientations. Rapid fluid-pressure fluctuations during faulting can cause the preferential partitioning of reduced gas phases from the ore fluid and are an effective method of orogenic ore-fluid oxidation. In addition, at different stages of the progressive fault-valve cycle, different gold-precipitation mechanisms are dominant. For example, fluid-rock interaction with rock-buffered reactions will be the dominant mechanism during pre-failure discharge of fluids from faults. Fluctuations in fluid pressure during, and immediately after, faulting can cause fluid-dominated processes such as phase separation and back-mixing of modified ore-fluid components. Any, or all, of these three gold-depositional mechanisms can induce oxidation in orogenic gold fluids under appropriate conditions.

Negative average $\delta^{34}\text{S}$ values and large variations in $\delta^{34}\text{S}$ values of ore-related pyrites in world-class orogenic gold deposits are interpreted to be the result of multiple mechanisms of gold precipitation within a single and widespread orogenic ore fluid (Ridley and Diamond 2000) in specific structural settings, rather than the result of different ore fluids. Magmatic fluids from shallow-level felsic intrusions, although not completely ruled out as an important source of oxidised ore fluids (cf. Cameron and Hattori 1987), do not appear to be necessary to account for negative $\delta^{34}\text{S}$ values of ore-related pyrites in orogenic gold deposits in the Eastern Goldfields Province. Available studies suggest, instead, that they pre-date gold mineralisation but induced early hematite or magnetite alteration that modified potential host rocks and made them more reactive to orogenic gold fluids.

Acknowledgements This study was part of the Ph.D. research of PFH (Hodkiewicz 2003) at the University of Western Australia, which was supported by an Australian Postgraduate Award (Industry) scholarship and was part of Australian Minerals Industry Research Association Project P511. Thanks to Keith Harris, manager of the Central Science Laboratory at the ARC Centre of Excellence in Ore Deposits, University of Tasmania, for assistance with sulphur isotope analyses. Special thanks also to Paul Kitto for logistical and analytical assistance and for helpful discussions and access to unpublished data. We are most grateful for the critical reviews of David Huston and John Walshe which resulted in a significantly improved paper.

References

- Allen CA (1986) Mineralisation controls and alteration of the Archaean quartz-monzonite-hosted Porphyry gold deposit. Unpublished Honours thesis, University of Western Australia, 73 p
- Allen CA (1987) The nature and origin of the Porphyry gold deposit, Western Australia. In: Ho SE, Groves DI (eds) Recent advances in understanding Precambrian gold deposits. Publication 11. Geology Department and Extension Service, University of Western Australia, Perth, pp 137–145
- Brown SM (2002) Structural and temporal evolution of a complex ore system: Cleo gold deposit, Eastern Goldfields Province, Western Australia. Unpublished Ph.D. thesis, University of Western Australia
- Brown SM, Tornatora P (2001) A review of geology and mining at the Cleo orebody, Sunrise Dam gold mine. In: Hagemann SG, Neumayr P, Witt WK (eds) World-class gold camps and deposits in the Eastern Yilgarn Craton, Western Australia, with special emphasis on the Eastern Goldfields Province. Western Australia Geological Survey Record 2001/17, pp 151–162
- Brown SM, Fletcher IR, Stein HJ, Snee LW, Groves DI (2002a) Geochronological constraints on pre-, syn- and postmineralisation events at the world-class Cleo gold deposit, Eastern Goldfields Province, Western Australia. *Econ Geol* 97:541–559
- Brown SM, Groves DI, Newton PG (2002b) Geological setting and mineralisation model for the Cleo gold deposit, Eastern Goldfields Province, Western Australia. *Miner Depos* 37:704–721
- Bucci LA (2001) An integrated temporal model of deformational, magmatic and hydrothermal mineralisation events at the amphibolite-hosted Chalice gold deposit, Yilgarn Craton, Western Australia. Unpublished Ph.D. thesis, University of Western Australia
- Cameron EM (1988) Archaean gold: relation to granulite formation and redox zoning in the crust. *Geology* 16:109–112
- Cameron EM, Hattori K (1987) Archaean gold mineralisation and oxidised hydrothermal fluids. *Econ Geol* 82:1177–1191
- Cassidy KF (1992) Archaean granitoid-hosted gold deposits in green schist to amphibolite facies terrains: a high P–T to low P–T depositional continuum equivalent to greenstone-hosted deposits. Unpublished Ph.D. thesis, University of Western Australia
- Cassidy KF, Bennett JM (1993) Gold mineralisation at the Lady Bountiful Mine, Western Australia: an example of a granitoid-hosted Archaean lode gold deposit. *Miner Depos* 28:388–408
- Cassidy KF, Groves DI, McNaughton NJ (1998) Late-Archaean granitoid-hosted lode-gold deposits, Yilgarn Craton, Western Australia: deposit characteristics, crustal architecture and implications for ore genesis. *Ore Geol Rev* 13:65–102
- Cater I (1992) The nature and controls on gold mineralisation in the Poseidon South gabbro-hosted deposit, Higginsville, Western Australia. Unpublished Honours thesis, University of Western Australia
- Champion DC, Cassidy KF (2002) Granites in the Leonora–Laverton transect area, northeastern Yilgarn craton, Western Australia. *Geoscience Australia Record* 2002/18, pp 13–30
- Clark ME (1987) The geology of the Victory gold mine, Kambalda, Western Australia. Unpublished PhD thesis, Queen's University
- Clark ME, Archibald NJ, Hodgson CJ (1986) The structural and metamorphic setting of the Victory gold mine, Kambalda, Western Australia. In: Macdonald AJ (ed) Gold '86: an international symposium on the geology of gold deposits: proceedings volume. Konsult International, Toronto, pp 243–254
- Clark ME, Carmichael DM, Hodgson CJ, Fu M (1989) Wall-rock alteration, Victory gold mine, Kambalda, Western Australia: processes and P–T–X conditions of metasomatism. In: Keays RR, Ramsay WRH, Groves DI (eds) The geology of gold deposits: the perspective in 1988. *Economic Geology Monograph* 6, pp 445–459
- Clout JMF (1989) Structural and isotopic studies of the Golden Mile gold-telluride deposit, Kalgoorlie, WA. Unpublished PhD thesis, Monash University
- Couture JF, Pilote P (1993) The geology and alteration patterns of a disseminated, shear zone-hosted mesothermal gold deposit: the Francoeur 3 Deposit, Rouyn-Noranda, Quebec. *Econ Geol* 88:1664–1684

- Cox SF (1999) Deformational controls on the dynamics of fluid flow in mesothermal gold systems. In: McCaffrey KJW, Lonergan L, Wilkinson J (eds) *Fractures, fluid flow and mineralisation*, Geological Society of London Special Publication 155. Geological Society of London, London, pp 123–140
- Donnelly TH, Lambert IB, Oehler DZ, Hallberg JA, Hudson DR, Smith JW, Bavinton OA, Golding L (1978) A reconnaissance study of stable isotope ratios in Archaean rocks from the Yilgarn Block, Western Australia. *J Geol Soc Austr* 24:409–420
- Drummond SE, Ohmoto H (1985) Chemical evolution and mineral deposition in boiling hydrothermal systems. *Econ Geol* 80:126–147
- Duuring P (2002) Structural and hydrothermal fluid controls on metallogenesis associated with Archaean granitoids in the Yilgarn Craton, Western Australia: evidence from the Jupiter and Tarmoola gold deposits. Unpublished PhD thesis, University of Western Australia
- Evans KA, Phillips GN, Powell R (2006) Rock-buffering of auriferous fluids in altered rocks associated with the Golden-Mile style mineralization, Kalgoorlie Gold Field, Western Australia. *Econ Geol* 101:805–817
- Gebre-Mariam M (1994) The nature and genesis of Archaean mesozonal to epizonal gold deposits of the Mt. Pleasant area, near Kalgoorlie, Western Australia. Unpublished Ph.D. thesis, University of Western Australia
- Golding SD, Groves DI, McNaughton NJ, Mikuck EJ, Sang JH (1990) Source of ore fluid and ore components: sulphur isotope studies. In: Ho SE, Groves DI, Bennett JM (eds) *Gold deposits of the Archaean Yilgarn Block, Western Australia: nature, genesis and exploration guides*. Publication 20. Geology Department and Extension Services, University of Western Australia, Perth, pp 259–262
- Groenewald PB, Riganti A (2004) East Yilgarn 1:100000 Geological Information Series—an explanatory note. Western Australia Geological Survey, Report 95, 58 p
- Groves DI, Goldfarb RJ, Robert F, Hart CJR (2003) Gold deposits in metamorphic belts: overview of current understanding, outstanding problems, future research, and exploration significance. *Econ Geol* 98:1–29
- Guha J, Lu HZ, Dube B, Robert F, Gagnon M (1991) Fluid characteristics of vein and altered wall rock in Archean mesothermal gold deposits. *Econ Geol* 86:667–684
- Hagemann SG (1992) The Wiluna lode-gold deposits, Western Australia: a case study of a high crustal level Archean lode-gold system. Unpublished PhD thesis, University of Western Australia
- Hagemann SG, Cassidy KF (2000) Archean orogenic lode gold deposits. *Soc Econ Geol Rev* 13:9–68
- Hagemann SG, Bateman R, Crowe D, Vielreicher RM (1999) In situ sulfur isotope composition of pyrites from the Fimiston- and Oryoa-style gold lodes in the Golden Mile Camp, Kalgoorlie: implications for sulfur source(s) and depositional processes. *Geological Society of America Abstracts with Programs* 31/7, p 32
- Hall GA, Wall VJ, Massey S (2001) Archean pluton-related (thermal aureole) gold: the Kalgoorlie exploration model. In: 2001—a hydrothermal odyssey. Townsville, EGRU, James Cook University Economic, Queensland, pp 66–67
- Harbi H (1997) Origin of the stockwork gold mineralisation at Kalgoorlie, Western Australia. Unpublished Ph.D. thesis, University of Western Australia
- Hattori K (1987) Magnetic felsic intrusions associated with Canadian Archean gold deposits. *Geology* 15:1107–1111
- Henly RW, Ellis AJ (1983) Geothermal systems, ancient and modern. *Earth Sci Rev* 19:1–50
- Ho SE, McNaughton NJ, Groves DI (1994) Criteria for determining initial lead isotopic compositions of pyrite in Archean lode-gold deposits: a case study at Victory, Kambalda, Western Australia. *Chem Geol* 111:57–84
- Hodge JL, Hagemann SG, Neumayr P (2005) Characteristics and evolution of hydrothermal fluids from the Archean orogenic New Celebration gold deposits, Western Australia. In: Mao J, Bierlein FP (eds) *Mineral deposit research: meeting the global challenge*. Proceedings of the Eighth Biennial SGA Meeting, Beijing. Springer, Heidelberg, pp 529–532
- Hodkiewicz PF (2003) The interplay between physical and chemical processes in the formation of world-class orogenic gold deposits in the Eastern Goldfields Province, Western Australia. Unpublished Ph.D. thesis, University of Western Australia
- Hronsky JMA (1993) The role of physical and chemical processes in the formation of gold ore-shoots at the Lancefield gold deposit, Western Australia. Unpublished Ph.D. thesis, University of Western Australia
- Huston DL, Power M, Gemmill JB, Large RR (1995) Design, calibration and geological application of the first operational Australian laser ablation sulphur isotope microprobe. *Aust J Earth Sci* 42:549–555
- Huston DL, Brauhart CW, Driehberg SL, Davidson GJ, Groves DI (2001) Metal leaching and inorganic sulfate reduction in volcanic-hosted massive sulfide mineral systems: evidence from the paleo-Archaean Panorama district, Western Australia. *Geology* 29:687–690
- Kent AJR (1994) Geochronological constraints on the timing of Archean gold mineralisation in the Yilgarn Craton, Western Australia. Unpublished Ph.D. thesis, Australia National University
- Kenworthy S, Hagemann SG (2005) Decoupled lamprophyric magmatism and gold mineralisation at the Archean Darlot lode gold deposit, Western Australia. In: Mao J, Bierlein FP (eds) *Mineral deposit research: meeting the global challenge*. Proceedings of the Eighth Biennial SGA Meeting, Beijing. Springer, Heidelberg, pp 987–990
- Kerrick R (1986) The stable isotope geochemistry of Au–Ag vein deposits in metamorphic rocks. In: Kyser TK (ed) *Mineralogical Association of Canada short course 13*. Mineralogical Association of Canada, Saskatoon, pp 287–336
- Kerrick R (1989) Archean gold: relation to granulite formation or felsic intrusions? *Geology* 17:1011–1015
- Lambert IB, Phillips GN, Groves DI (1984) Sulphur isotope compositions and genesis of Archean gold mineralisation, Australia and Zimbabwe. In: Foster RP (ed) *Gold '82: The geology, geochemistry and genesis of gold deposits*. A.A. Balkema, Rotterdam, pp 373–387
- Loucks RR, Mavrogenes JA (1999) Gold solubility in supercritical hydrothermal brines measured in synthetic fluid inclusions. *Science* 284:2159–2163
- Marini L, Chiappini V, Cioni R, Cortecchi G, Dinelli E, Principe C, Ferrar G (1998) Effect of degassing on sulfur contents and $\delta^{34}\text{S}$ values in Somma-Vesuvius magmas. *Bull Volcanol* 60:187–194
- McCuaig TC (1996) The genesis and evolution of lode gold mineralisation and mafic host lithologies in the late-Archaean Norseman Terrane, Yilgarn Block, Western Australia. Unpublished Ph.D. thesis, University of Saskatchewan
- McCuaig TC, Kerrich R (1998) P–T–t-deformation-fluid characteristics of lode gold deposits: evidence from alteration systematics. *Ore Geol Rev* 12:381–453
- McCuaig TC, Kerrich R, Groves DI, Archer N (1993) The nature and dimensions of regional and local gold-related hydrothermal alteration in tholeiitic metabasalts in the Norseman goldfields: the missing link in a crustal continuum of gold deposits? *Miner Depos* 28:420–435

- McNaughton NJ, Mueller AG, Groves DI (2006) The age of the giant Golden Mile deposit, Kalgoorlie, Western Australia: SHRIMP ion-microprobe zircon and monazite U–Pb geochronology of a syn-mineralization lamprophyre dike. *Econ Geol* 100:1363–1388
- Mikucki JA (1997) Contrasting fluid sources and mineralisation styles in the Great Eastern Archaean lode-gold deposits, Lawlers, Western Australia. Unpublished Ph.D. thesis, University of Western Australia
- Mikucki EJ (1998) Hydrothermal transport and depositional processes in Archean lode-gold systems: a review. *Ore Geol Rev* 13:307–321
- Mikucki EJ, Groves DI (1990) Gold transport and depositional models. In: Ho SE, Groves DI, Bennett JM (eds) Gold deposits of the Archaean Yilgarn Block, Western Australia: nature, genesis and exploration guides. Publication 20. Geology Department and Extension Services, University of Western Australia, Perth, pp 278–284
- Mikucki EJ, Ridley JIR (1993) The hydrothermal fluid of Archaean lode-gold deposits at different metamorphic grades: compositional constraints from ore and wall rock alteration assemblages. *Miner Depos* 28:469–481
- Mueller AG (1990) The nature and genesis of high- and medium-temperature Archaean gold deposits in the Yilgarn block, Western Australia, including a specific study of scheelite-bearing gold skarn deposits. Unpublished Ph.D. thesis, University of Western Australia
- Neall FB, Phillips GN (1987) Fluid-wall rock interaction in an Archaean hydrothermal gold deposit: a thermodynamic model for the Hunt Mine, Kambalda. *Econ Geol* 82:1679–1694
- Neumayr P, Petersen KJ, Gauthier L, Hodge J, Hagemann SG, Walshe JL, Prendergast K, Conners K, Horn L, Frikken P, Roache A, Blewett R (2005) Mapping of hydrothermal alteration and geochemical gradients as a tool for conceptual targeting: St. Ives gold camp, Western Australia. In: Mao J, Bierlein FP (eds) Mineral deposit research: meeting the global challenge. Proceedings of the Eighth Biennial SGA Meeting, Beijing. Springer, Heidelberg, pp 1479–1482
- Nguyen PT (1997) Structural controls on gold mineralisation of the Revenge deposit and its setting in the Lake Lefroy area, Kambalda, Western Australia. Unpublished Ph.D. thesis, University of Western Australia
- Nguyen PT, Cox SF, Harris LB, Powell CM (1998) Fault-valve behaviour in optimally oriented shear zones: an example at the Revenge gold mine, Kambalda, Western Australia. *J Struct Geol* 20:1625–1640
- Ohmoto H (1972) Systematics of sulfur and carbon isotopes in hydrothermal ore deposits. *Econ Geol* 67:551–578
- Ohmoto H (1986) Stable isotope geochemistry of ore deposits. In: Valley JW, Taylor HPJ, O'Neil JR (eds) Stable isotopes in high temperature geological processes. Reviews in mineralogy. Mineralogical Society of America, Chantilly, pp 491–559
- Ohmoto H, Goldhaber MB (1997) Sulfur and carbon isotopes. In: Barnes HL (ed) Geochemistry of hydrothermal ore deposits. Wiley, New York, pp 517–612
- Ohmoto H, Rye RO (1979) Isotopes of sulfur and carbon. In: Barnes HL (ed) Geochemistry of hydrothermal ore deposits. Wiley, New York, pp 509–567
- Ojala VJ (1995) Structural and depositional controls on gold mineralisation at the Granny Smith Mine, Laverton, Western Australia. Unpublished PhD thesis, University of Western Australia
- Palin JM, Xu Y (2000) Gilt by association? Origins of pyritic gold ores in the Victory mesothermal gold deposit, Western Australia. *Econ Geol* 95:1627–1634
- Palin JM, Heath CJ, Campbell IH (2001) Wall rock carbonation and large mesothermal gold deposits: coincidence or cause? In: 2001—a hydrothermal odyssey, Townsville, EGRU, James Cook University, Queensland, pp 160–161
- Phillips GN, Groves DI (1983) The nature of Archaean gold-bearing fluids as deduced from gold deposits of Western Australia. *J Geol Soc Aust* 30:25–39
- Phillips GN, Groves DI (1984) Fluid access and fluid–wall rock interaction in the genesis of the Archaean gold–quartz vein deposit at Hunt Mine, Kambalda, Western Australia. In: Foster RP (ed) Gold '82: the geology, geochemistry and genesis of gold deposits. A.A. Balkema, Rotterdam, pp 389–416
- Phillips GN, Groves DI, Neall FB, Donnelly TH, Lambert IB (1986) Anomalous sulfur isotope compositions in the Golden Mile, Kalgoorlie. *Econ Geol* 81:2008–2015
- Phillips GN, Groves DI, Kerrich R (1996) Factors in the formation of the giant Kalgoorlie gold deposit. *Ore Geol Rev* 10:295–317
- Polito P (1999) Exploration implications predicted by the distribution of carbon–oxygen–hydrogen gases above and within the Junction gold deposit, Kambalda, Western Australia. Unpublished Ph.D. thesis, University of Adelaide
- Qui Y, McNaughton NJ (1999) Source of Pb in orogenic lode-gold mineralisation: Pb isotope constraints from deep crustal rocks from the southwestern Archaean Yilgarn craton, Australia. *Miner Depos* 34:366–381
- Ridley JR, Diamond LW (2000) Fluid chemistry of orogenic lode gold deposits and implications for genetic models. *Soc Econ Geol Rev* 13:141–162
- Robert F, Boullier AM, Firdaus K (1995) Gold–quartz veins in metamorphic terranes and their bearing on the role fluids in faulting. *J Geophys Res* 100:12861–12879
- Roberts RG (1987) Ore deposit models: Archean lode gold deposits. *Geosci Can* 14:37–52
- Roberts DE, Elias M (1990) Gold deposits of the Kambalda-St Ives region. In: Hughes FE (ed) Geology of the mineral deposits of Australia and Papua New Guinea. Australasian Institute of Mining and Metallurgy Monograph 14, pp 479–491
- Robinson BW, Kusakabe M (1975) Quantitative preparation of sulfur dioxide for 34S/32S analyses from sulfides by combustion with cuprous oxide. *Anal Chem* 47:1179–1181
- Ross A (2002) Genesis of the Kanowna Belle gold deposit, Western Australia: implications for Archean metallogeny in the Yilgarn Craton. Unpublished Ph.D. thesis, University of Western Australia
- Rye RO (1993) SEG Distinguished Lecture: the evolution of magmatic fluids in the epithermal environment: the stable isotope perspective. *Econ Geol* 88:733–753
- Salier BP, Groves DI, McNaughton NJ, Fletcher IR (2004) The world-class Wallaby gold deposit, Laverton, Western Australia: an orogenic-style overprint on a magmatic–hydrothermal magnetite–calcite alteration pipe? *Miner Dep* 39:473–494
- Salier BP, Groves DI, McNaughton NJ, Fletcher IR (2005) Geochronological and stable isotope evidence for widespread gold mineralization from deep-seated fluid source at ca 2.65 Ga in the Laverton Gold Province, Western Australia. *Econ Geol* 100:1363–1388
- Secombe PK, Groves DI, Marston RJ, Barrett FM (1981) Sulfide paragenesis and sulfur mobility in Fe–Ni–Cu sulfide ores at Lunnon and Juan Main shoots, Kambalda: textural and sulfur isotopic evidence. *Econ Geol* 76:1675–1685
- Seward TM (1973) Thio complexes of gold and the transport of gold in hydrothermal ore solutions. *Geochim Cosmo Acta* 37:379–399
- Sibson RH, Robert F, Poulsen H (1988) High angle faults, fluid pressure cycling and mesothermal gold–quartz deposits. *Geology* 16:551–555

- Skwarnecki MS (1990) The regional setting and genesis of Archaean gold mineralisation at Harbour Lights, Leonora, Western Australia. Unpublished Ph.D. thesis, University of Western Australia
- Townsend DB, Mai G, Morgan WR (2000) Mines and mineral deposits of Western Australia: digital extract from MINEDEX—an explanatory note. Geological Survey of Western Australia Record 2000/13, 28 p
- Uemoto T, Ridley J, Mikucki E, Groves DI (2002) Fluid chemical evolution as a factor in controlling the distribution of gold at the Archean Golden Crown lode gold deposit, Murchison Province, Western Australia. *Econ Geol* 97:1227–1248
- Vanderhor F, Groves DI (1998) Systematic documentation of Archaean gold deposits of the Yilgarn block. MERIWA Report 193. Minerals and Energy Resource Institute of Western Australia, Perth
- Vearncombe JR, Barley ME, Eisenlohr BN, Groves DI, Houston SM, Skwarnecki MS, Grigson MW, Partington GA (1989) Structural controls on gold mineralization: examples from the Archean terranes of southern Africa and Western Australia. *Econ Geol Monogr* 6:124–134
- Vielreicher NM, Groves DI, McNaughton NJ, Snee LW (2007) Timing of gold mineralisation at Kalgoorlie, Western Australia. In: Andrew CJ (ed.) Proceedings of the Ninth Biennial SGA Meeting: Mineral Exploration and Research: Digging Deeper, Dublin. Irish Association for Economic Geology, pp 341–344
- Walsh JF, Kesler SE, Duff D, Cloke PL (1988) Fluid inclusion geochemistry of high-grade, vein-hosted gold ore at the Pamour mine, Porcupine camp, Ontario. *Econ Geol* 83:1347–1367
- Walshe JL, Hobbs BE, Hall GC, Ord A (1999) Towards an understanding of giant gold systems. In: Society of Mining Engineers, Metallurgists and Explorationists Annual Meeting Conference Proceedings, Denver, pp 1–6
- Watchorn RB (1998) Kambalda-St Ives gold deposits. In: Berkman DA, Mackenzie DH (eds) Geology of Australian and Papua New Guinean mineral deposits. Australasian Institute of Mining and Metallurgy Monograph 22, pp 243–254
- Williams H (1994) The lithological setting and controls on gold mineralisation in the Southern Ore Zone of the Hampton-Boulder gold deposit, New Celebration gold mine, Western Australia. Unpublished Honours thesis, University of Western Australia
- Witt WK (1992a) Gold deposits of the Kalgoorlie–Kambalda–St. Ives areas, Western Australia: Part 3 of a systematic study of the gold mines of the Menzies–Kambalda region. Geological Survey of Western Australia Record 1992/15, 107 p
- Witt WK (1992b) Gold deposits of the Mt. Pleasant–Ora Banda areas, Western Australia: Part 2 of a systematic study of the gold mines of the Menzies–Kambalda region. Geological Survey of Western Australia Record 1992/14, 103 p
- Witt WK (1993) Gold mineralisation in the Menzies–Kambalda region, Eastern Goldfields, Western Australia. Geological Survey of Western Australia Report 39, 65 p
- Witt WK (1995) Phase separation (boiling) as a mechanism for deposition of gold in low-iron host rocks, Yarri mining district, Eastern Goldfields Province. In: Nowak IR (ed) Geological Survey of Western Australia Annual Review 1995–96, pp 149–155
- Witt WK, Vanderhor F (1998) Diversity within a unified model for Archaean gold mineralization in the Yilgarn Craton of Western Australia: an overview of the late-orogenic, structurally-controlled gold deposits. *Ore Geol Rev* 13:29–64
- Xu Y (1999) The stable isotope and trace element geochemistry of the Victory gold deposit, Western Australia. Unpublished Ph.D. thesis, Australian National University
- Zhang X, Spry PG (1994) FO2PH: a quickBASIC program to calculate mineral stabilities and sulphur isotope contours in log fO₂-pH space. *Mineral and Petrol* 50:287–291